Quantum theory of bilayer quantum Hall smectics

Emiliano Papa,[1] John Schliemann,[1,2] A. H. MacDonald,[1] and Matthew P. A. Fisher[3]
[1]*Department of Physics, The University of Texas, Austin, Texas 78712*
[2]*Department of Physics and Astronomy, University of Basel, CH-4056 Basel, Switzerland*
[3]*Kavli Institute for Theoretical Physics, University of California at Santa Barbara, Santa Barbara, California 93106*
(Received 6 September 2002; published 25 March 2003)

Mean-field theory predicts that bilayer quantum Hall systems at odd integer total filling factors can have stripe ground states, in which the top Landau level is occupied alternately by electrons in one of the two layers. We report on an analysis of the properties of these states based on a coupled-Luttinger-liquid description that is able to account for quantum fluctuations of charge-density and position along each stripe edge. The soft modes associated with the broken symmetries of the stripe state lead to an unusual coupled-Luttinger-liquid system with strongly enhanced low-temperature heat capacity and strongly suppressed low-energy tunneling density of states. We assess the importance of the intralayer and interlayer backscattering terms in the microscopic Hamiltonian, which are absent in the Luttinger liquid description, by employing a perturbative renormalization group approach which rescales time and length along but not transverse to the stripes. With interlayer backscattering interactions present the Luttinger-liquid states are unstable either to an incompressible striped state that has spontaneous interlayer phase coherence and a sizable charge gap even at relatively large layer separations, or to Wigner crystal states. Our quantitative estimates of the gaps produced by backscattering interactions are summarized in Fig. 11 by a schematic phase diagram intended to represent predicted experimental findings in very high mobility bilayer systems at dilution refrigerator temperatures as a function of layer separation and bilayer density balance. We predict that the bilayer will form incompressible isotropic interlayer phase-coherent states for small layer separations, say $d \leqslant 1.5\ell$. At larger interlayer spacings, however, the bilayer will tend to form one of several different anisotropic states depending on the layer charge balance, which we parametrize by the fractional filling factor ν contributed by one of the two layers. For large charge imbalances (ν far from 1/2), we predict states in which anisotropic Wigner crystals form in each of the layers. For ν closer to 1/2, we predict stripe states that have spontaneous interlayer phase-coherence and a gap for charged excitations. These states should exhibit the quantum Hall effect for current flowing within the layers and also the giant interlayer tunneling conductance anomalies at low bias voltages that have been observed in bilayers when the $N=0$ Landau level is partially filled. When the gaps produced by backscattering interactions are sufficiently small, the phenomenology observed at typical dilution fridge temperatures will be that of a smectic metal, anisotropic transport without a quantum Hall effect. For stripe states in the $N=2$ Landau level, this behavior is expected over a range of bilayer charge imbalances on both sides of $\nu=1/2$.

DOI: 10.1103/PhysRevB.67.115330 PACS number(s): 73.40.Gk, 73.43.Lp, 73.20.Mf

I. INTRODUCTION

The recent discovery of strongly anisotropic transport in single-layer quantum Hall systems near half-odd integer filling factors[1–3] has attracted much experimental[4] and theoretical[5] interest. Transport anisotropies have been observed in single two-dimensional (2D) electron gas layers at half filling of Landau levels with index $N \geqslant 2$, i.e., at filling factors $\nu = 9/2, 11/2, \ldots$. This effect is commonly ascribed to the formation of striped charge-density-wave phases, predicted on the basis of the Hartree-Fock calculations by Koulakov *et al.*[6] and by Moessner and Chalker[7] with additional theoretical support from subsequent exact diagonalization[8] and DMRG[9] numerical studies. The stripe state is a consequence of the form factors that arise in describing interactions between electrons in higher kinetic-energy Landau-level orbitals and allow density waves to form in cyclotron-orbit-center coordinates that have a very small electron-density-wave amplitude, and therefore little electrostatic energy penalty.

The physics of quantum Hall systems is enriched by the additional degrees of freedom that appear in bilayer systems,[10] in which two 2D electron layers have a separation d small enough that their interactions have consequences. For total filling factor $\nu_T = 1$ and other odd integer total filling factors, interlayer interactions can lead to a state with spontaneous phase coherence[11] between the layers and a charge gap that is revealed experimentally[12] by the quantum Hall effect. Further spectacular experimental manifestations of spontaneous phase coherence were revealed very recently in 2D to 2D tunneling and Hall drag experiments by Eisenstein and collaborators.[13] In tunneling studies spontaneous coherence is signaled by a sharp zero bias peak in the differential conductance between the layers. As the ratio of d to the magnetic length ℓ is reduced experimentally, the conductance peak appears to develop continuously starting at a critical value of d/ℓ that is consistent with earlier experimental anomalies[12] attributed to spontaneous coherence and with mean-field-theory estimates of the critical layer separation[12] at which coherence is expected to develop. These experiments are still not understood quantitatively and raise a number of interesting issues in nonequilibrium collective transport theory that have stimulated a growing body of theoretical[14] work.

Since balanced bilayer systems at large odd integer total filling factor ($\nu_T \geqslant 9$) are composed of 2D layers that, if isolated, would show stripe-state behavior, it is natural to consider the possible interplay and competition between the formation of striped phases in each 2D layer and the development of spontaneous interlayer phase coherence. These issues have been investigated in several recent theoretical papers,[15–17] and it has been argued[17] that they may be relevant for understanding a recent observation of resistance anisotropy at integer filling factor by Pan *et al.*[18] In the present paper we extend earlier work by two of the present authors[19] on smectic states in single layers to the case of bilayer systems. The approach we take is one that is intended to be valid when quantum fluctuation corrections to the stripe states predicted by the Hartree-Fock theory are weak on microscopic length scales, although as we discuss at length they inevitably alter the ultimate physics at very low energies and temperatures and the behavior of correlation functions at long distances. Since stripe states occur as extrema of the Hartree-Fock energy functional for any orbital Landau-level index, not only for $N \geqslant 2$ where the states are seen experimentally, and are in fact *always* unstable to the formation of the Wigner crystal states in mean-field theory, it is evident that we must appeal in part to experiment to judge when our starting assumption is valid.[5,6,20]

In describing stripe states it is convenient to use a Landau gauge basis with single-particle states extended in the direction along the stripes, which we choose to be the $\hat{x}$ direction, and labeled by a one-dimensional wave vector k that is proportional to the guiding center, along which the wavefunction's y coordinate is localized, $Y = k\ell^2$. For balanced bilayers, the stripe states that occur in the Hartree-Fock theory are occupation number eigenstates in this representation, with the valence Landau-level Landau gauge states occupied by top and bottom layer electrons in alternating stripes. In the Hartree-Fock approximation, the low-energy excitations of the stripe states consist of coupled particle-hole excitations along each edge of top and bottom layer stripes. These degrees of freedom are conveniently described using the bosonization techniques familiar from the theory of one-dimensional electron systems.[21] Our approach is partly in the spirit of Fermi-liquid theory in that we assume that the Hilbert space of low-energy excitations can be placed in one-to-one correspondence with those that occur in the Hartree-Fock theory. When quantum fluctuations are too strong our approach will not be useful; for example, it cannot predict either the fact that the lowest Landau-level isolated layers have composite-fermion liquid rather than stripe ground states, or the likelihood of *bubble*[6] rather than stripe states far away from half filling. Our approach to stripe-state physics is similar to that taken first by Fradkin and Kivelson.[22] For the case of monolayers, the microscopic basis of the coupled-Luttinger-liquid model for quantum Hall stripe states was carefully examined by Lopatnikova *et al.*[23] and other properties of quantum Hall stripe states have been addressed by Barci *et al.*,[24] Wexler and Dorsey,[25] and Radzihovsky and Dorsey.[26]

Our paper is organized as follows. In Sec. II we review the coupled-Luttinger-liquid model for quantum Hall stripe states and discuss its application to the bilayer case. The model rests fundamentally on the assumption that the excitation spectrum of bilayer stripe states may be placed in one-to-one correspondence with that of the Hartree-Fock picture; for bilayers, this assumption implies that the degrees of freedom at each stripe edge are those of a one-dimensional electron gas. Our analysis of the low-energy long-wavelength physics examines this subspace of the microscopic many-particle Hilbert space and includes *forward-scattering* terms in the Hamiltonian that create and destroy particle-hole excitations at the stripe edges, and *backscattering* terms that scatter electrons between chiral one-dimensional electron-gas branches. Since the microscopic amplitude of backscattering processes is weak, they can often be neglected at experimentally accessible temperatures. When only forward-scattering terms are included, the Hamiltonian can be solved exactly using bosonization and is formally equivalent to that of a system of coupled one-dimensional electron gases. The quantum smectic broken symmetry character of the electronic state is reflected, however, in the coupled-Luttinger-liquid interaction parameters and results in enhanced fluctuations. The properties of this bilayer smectic state are discussed in Sec. III. The behavior of the one-particle Green's functions at the smectic fixed point, carefully addressed by Lopatnikova *et al.*[23] for the single-layer case, is discussed for the bilayer. We find that, as in the single-layer case, the one-particle Green's function does not exhibit the power-law behavior that is generic for weakly-coupled Luttinger-liquids and instead vanishes faster than any power law at large distances, implying strongly suppressed tunneling at low energies. The enhanced importance of quantum fluctuations is a consequence of the invariance of the model's Luttinger-liquid Hamiltonian under a simultaneous translation of all stripes. Backscattering interactions are addressed in Sec. IV, using a perturbative renormalization group (RG) approach. As in the single-layer case we find that backscattering interactions are always relevant. *The gapless Hartree-Fock smectic state cannot be the true ground state in either single-layer or bilayer quantum Hall systems.* Instead, we conclude that except at relatively large layer separations, interlayer interactions induce a ground state that has spontaneous interlayer phase coherence. This state would be signaled experimentally by the simultaneous occurrence of an integer quantum Hall effect and anisotropic finite-temperature transport, something that has not been seen in single-layer systems. Where intralayer interactions are more important, they drive the system to a state with an anisotropic Wigner crystal in each layer. We argue that both types of interactions lead to charge gaps and to integer quantum Hall effects and estimate the size of the resulting energy gaps. According to our estimates, the gap created by interlayer backscattering will be large enough to be observable out to surprisingly large layer separations. The effect of finite tunneling between the layers is also addressed in Sec. IV. Finally in Sec. V we discuss several interesting theoretical issues that arise from this work. We comment explicitly on inconsistencies between the conclusions that have been reached by different researchers on the question of smectic state stability in the single-layer case. We also address the suggestion[24] that the enhanced quantum fluctuations that fol-

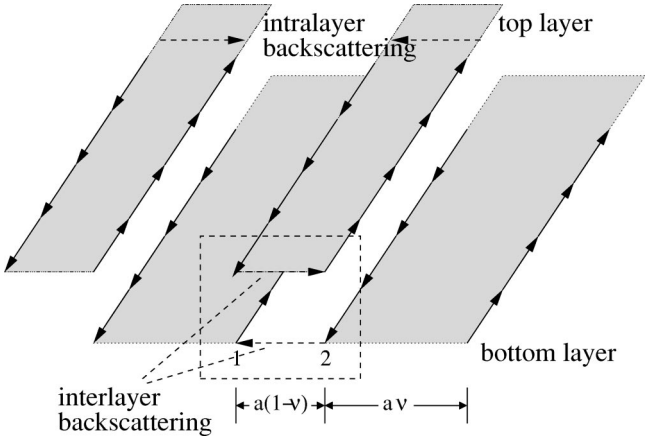

FIG. 1. Schematic illustration of the Hartree-Fock bilayer smectic state. The shaded areas are electron stripes whose edges are chiral Luttinger-liquids as denoted by the solid arrows. Each electron (hole) stripe in one layer faces a hole (electron) stripe in the other. The average filling factor of the highest occupied Landau-level is ν while that in the top layer is $1-\nu$, giving a total filling factor $\nu_T=1$. In the convention used here, a rung pair consists of the edges of an electron stripe in the top layer and an hole stripe in the bottom layer. The right-moving and left-moving chiral quasiparticle branches of each element of a rung pair are localized in opposite layers and denoted by $\lambda=1,2$. The momentum-conserving backscattering interactions not present in the Luttinger-liquid model, discussed in this section, include both interlayer and intralayer processes which have different behavior. The figure illustrates interlayer and intralayer backscattering processes with the smallest possible momentum transfer.

low from the broken translational symmetry of the starting Hartree-Fock state may invalidate our perturbative renormalization group analysis for backscattering interactions.

II. THE MODEL

A. Coupled-Luttinger-liquid model energy functional

In Hartree-Fock theory the smectic bilayer state at total filling factor $\nu_T=1$ is a single Slater determinant where the occupation of guiding-center modes in a Landau-level of index $N\in\{0,1,2,\ldots\}$ alternates between the layers with period a, as depicted schematically in Fig. 1. The lower index Landau levels are assumed to be frozen in filled states and higher index in empty states, allowing them to be neglected in the following. Each stripe has chiral left-moving and right-moving branches of quasiparticle edge states, localized in opposite layers, allowing the low-energy degrees of freedom of each electron stripe to be mapped to those of a one-dimensional electron gas. We consider the general case of a *biased* double-layer system where the width of the stripes in one layer is $a\nu$ while that in the other layer is $a(1-\nu)$, $\nu\in[0,1]$. As indicated in the figure, for $\nu\neq 0.5$ the system has two types of stripe edges, distinguished by the direction of their closest neighbor. In the following we refer to a pair of chiral stripe edges one above the other in each layer as a *rung*, and the two closest such rungs as a *rung pair*.

Small fluctuations in the positions and charge densities of the stripes can be described in terms of particle-hole excitations near the stripe edges. The residual interactions, ignored in the Hartree-Fock theory, which act on energy states fall into two classes: *forward*-scattering interactions which conserve the number of electrons on each edge of every stripe, and *backward*-scattering processes which do not. The quantum smectic model includes forward-scattering processes only. Backscattering processes involve large momentum transfer and their bare matrix elements will be smaller in magnitude (see below). We treat their effects perturbatively, using a renormalization group approach to account for the infrared divergences ubiquitous in quasi-one-dimensional electron systems. The smectic state is stable only if the backscattering interactions are irrelevant.

The *classical* quadratic Hamiltonian which describes the energetics of small stripe edge fluctuations has the following general form:[19]

$$\mathcal{H}_0=\frac{1}{2\ell^2}\int dx\int dx'\sum_{j,k=-\infty}^{\infty}\sum_{\lambda,u=1,2}\sum_{\alpha,\beta=R,L}[u^{\lambda}_{j\alpha}(x)K^{\lambda\mu}_{\alpha\beta}\times(x-x',j-k)u^{u}_{k\beta}(x')], \tag{1}$$

where the indices j and k label rung pairs, λ and u are the two different rungs within a rung pair, α and β are the right- or left-moving chiral edges within a single rung, and x, x' are positions along the stripes. In this equation, $u^{\lambda}_{j\alpha}$ is the transverse displacement of the edge (j,λ,α) from its classical ground-state location.

In Eq. (1), the linear charge-density associated with an edge displacement is $\rho^{\lambda}_{j\alpha}(x)=\alpha n u^{\lambda}_{j\alpha}(x)$, where n is the two-dimensional electron density inside the stripes $n=1/2\pi l^2$ and $\alpha=-,+$, or L,R, for the left, right, moving fermions, respectively. It follows from symmetry considerations that the elastic kernel satisfies the following equalities,

$$K^{\lambda u}_{\alpha\beta}(j)=K^{\lambda u}_{\beta\alpha}(j)=K^{\lambda u}_{(-\alpha)(-\beta)}(j)=K^{\lambda u}_{\alpha\beta}(-j), \tag{2}$$

which allow the Hamiltonian to be rewritten into sums and differences of the positions of left- and right-going branch edges,

$$\mathcal{H}_0=\frac{1}{8l^4}\int dx\int dx'\sum_{j,k=-\infty}^{\infty}\sum_{\lambda,u=1,2}[[u^{\lambda}_{j,R}(x)+u^{\lambda}_{j,L}(x)]\times K^{\lambda\mu}_{\mathrm{p}}(x-x',j-k)[u^{u}_{k,R}(x')+u^{u}_{k,L}(x')]+[u^{\lambda}_{j,R}(x)-u^{\lambda}_{j,L}(x)]K^{\lambda\mu}_{\mathrm{c}}(x-x',j-k)[u^{u}_{k,R}(x')-u^{u}_{k,L}(x')]], \tag{3}$$

where

$$K^{\lambda\mu}_{\mathrm{p}}(x,j)=\ell^2\sum_{\alpha\beta}K^{\lambda\mu}_{\alpha\beta}(x,j), \tag{4}$$

$$K^{\lambda\mu}_{\mathrm{c}}(x,j)=\ell^2\sum_{\alpha\beta}\alpha\beta K^{\lambda\mu}_{\alpha\beta}(x,j). \tag{5}$$

We regard the first term in this Hamiltonian as the contribution from fluctuations in the *position* of the rungs while the second term is the contribution from fluctuations of their

charge densities. (The total filling factor varies locally when left- and right-going branch edges do not move together.) These two terms are analogous, respectively, to current and charge terms in the effective Hamiltonian of a conventional one-dimensional electron gas. The calculations we perform here will require only the long-wavelength limits of the $x-x'$ dependence of elastic kernel in this Hamiltonian, which we estimate using a weak-coupling approximation that we discuss below.

B. Bosonization

This Hamiltonian is quantized by recognizing that charge and position fluctuations result from particle-hole excitations at the edges of chiral quasiparticle branches, just as in an ordinary one-dimensional electron system. The real spin is frozen due to the presence of strong perpendicular magnetic field and as a result we bosonize according to spinless bosonization scheme.[21] It follows from standard arguments that

$$[\rho^{\lambda}_{j,\alpha}(x),\rho^{u}_{k,\beta}(x')]=\frac{i}{2\pi}\delta_{\lambda,u}\delta_{\alpha,\beta}\delta_{j,k}\partial_x\delta(x-x'). \quad (6)$$

In terms of Fermion creation and annihilation operators

$$\rho^{\lambda}_{jR}(x)=:R^{\lambda\dagger}_j(x)R^{\lambda}_j(x):=R^{\lambda\dagger}_j(x)R^{\lambda}_j(x)-\langle R^{\lambda\dagger}_j(x)R^{\lambda}_j(x)\rangle, \quad (7)$$

$$\rho^{\lambda}_{jL}(x)=:L^{\lambda\dagger}_j(x)L^{\lambda}_j(x):=L^{\lambda\dagger}_j(x)L^{\lambda}_j(x)-\langle L^{\lambda\dagger}_j(x)L^{\lambda}_j(x)\rangle, \quad (8)$$

with $\lambda\in\{1,2\}$ denoting the rung in rung pair j and R, L, labeling right and left movers at the stripe edges.

The low-energy Hamiltonian is more conveniently described in terms of boson fields. The right- and left-moving fermionic fields on the left stripe edge of rung pair j are given by

$$\psi^1_{jR}(x)=e^{i[b(j-1/2)-k_F]x}R^1_j(x), \quad (9)$$

while those on the right are given by

$$\psi^2_{jR}(x)=e^{i[b(j-1/2)+k_F]x}R^2_j(x). \quad (10)$$

The above equations hold similarly for the left movers with the only change $R\to L$. Here $b=a/l^2$ is the width in k space of a rung and $k_F=a\nu/2l^2$ is the Fermi wave vector for the bottom layer stripes. The right and left slow fields can be expressed in terms of boson fields as in conventional one-dimensional electron systems:

$$R^{\lambda}_j(x)=\frac{1}{\sqrt{2\pi}}e^{i\phi^{\lambda}_{j,R}(x)}, \quad L^{\lambda}_j(x)=\frac{1}{\sqrt{2\pi}}e^{i\phi^{\lambda}_{j,L}(x)}, \quad (11)$$

where $\phi^{\lambda}_{j,R}(x)$ and $\phi^{\lambda}_{j,L}(x)$ are the chiral components of the bosonic field $\Phi^{\lambda}_j(x)=[\phi^{\lambda}_{j,R}(x)+\phi^{\lambda}_{j,L}(x)]/2$.

In terms of the bosonic fields the chiral currents take the following form,

$$\rho^{\lambda}_{j\alpha}(x)=-\frac{\alpha}{2\pi}\partial_x\phi^{\lambda}_{j,\alpha}(x). \quad (12)$$

Introducing the dual field $\Theta^{\lambda}_j(x)=[\phi^{\lambda}_{j,R}(x)-\phi^{\lambda}_{j,L}(x)]/2$ the position and charge variables U^{λ}_j, U'^{λ}_j, of the two-edge system can be expressed as $U^{\lambda}_j=-l^2\partial_x\Phi^{\lambda}_j$ and $U'^{\lambda}_j=-l^2\partial_x\Theta^{\lambda}_j$. This shows that the field Φ is related to the position fluctuations of the two-edge system whereas Θ is related with their charge-density fluctuations.

The field Φ and the dual field Θ satisfy the following commutation relation,

$$[\Theta^{\lambda}_j(x),\partial_{x'}\Phi^{u}_k(x')]=-i\pi\delta_{j,k}\delta_{\lambda,u}\delta(x-x') \quad (13)$$

(The fields $\Theta/\sqrt{\pi}$ and $-\partial_x\Phi/\sqrt{\pi}$ are canonical conjugates). In terms of these new fields the Hamiltonian takes the following form,

$$\mathcal{H}_0=\frac{1}{2}\int dxdx'\sum_{j,k}[\partial_x\Phi^{\lambda}_j(x)K^{\lambda u}_{\Phi}(x-x',j-k)\partial_{x'}\Phi^{u}_k(x') + \partial_x\Theta^{\lambda}_j(x)K^{\lambda u}_{\Theta}(x-x',j-k)\partial_{x'}\Theta^{u}_k(x')], \quad (14)$$

whereas the Fourier transform of the corresponding action

$$\mathcal{S}_0=\frac{i}{\pi}\int dxd\tau\sum_j\sum_{\lambda}(\partial_x\Phi^{\lambda}_j)\partial_\tau\Theta^{\lambda}_j+\int d\tau\mathcal{H}_0 \quad (15)$$

reads

$$\mathcal{S}_0=\int_{\mathbf{q},\omega}\Bigg[\sum_{\lambda}\left(\frac{i}{\pi}q_x\Phi^{\lambda *}(\mathbf{q},\omega)\omega\Theta^{\lambda}(\mathbf{q},\omega)\right) + \frac{1}{2}\sum_{\lambda,u}(q_x^2\Phi^{\lambda *}(\mathbf{q},\omega)K^{\lambda\mu}_{\Phi}(\mathbf{q})\Phi^{u}(\mathbf{q},\omega) + q_x^2\Theta^{\lambda *}(\mathbf{q},\omega)K^{\lambda\mu}_{\Theta}(\mathbf{q})\Theta^{u}(\mathbf{q},\omega))\Bigg]. \quad (16)$$

Here we have employed the shorthand notation

$$\int_{\mathbf{q},\omega}=\int_{-\Lambda}^{\Lambda}\frac{dq_x}{2\pi}\int_{-\pi/a}^{\pi/a}\frac{dq_y a}{2\pi}\int_{-\infty}^{\infty}\frac{d\omega}{2\pi} \quad (17)$$

with $\Lambda\sim 1/\ell$ a high-momentum cutoff, and have adopted the following Fourier-transform conventions:

$$F_j(x,\tau)=\int_{\mathbf{q},\omega}e^{i(q_x x+q_y aj-\omega\tau)}F(\mathbf{q},\omega), \quad (18)$$

$$F(\mathbf{q},\omega)=\int dxd\tau\sum_j e^{-i(q_x x+q_y aj-\omega\tau)}F_j(x,\tau). \quad (19)$$

The Quantum Field Theory applies for distances larger than l and as a result the q_x integration has to be cut off by $\pm 2\pi/l$. In Eq. (16) the kernel matrices $K_{\Phi}(\mathbf{q})$ and $K_{\Theta}(\mathbf{q})$ are the Fourier transforms of

$$K^{\lambda\mu}_{\Phi}(x,j)=K^{\lambda\mu}_{\mathrm{p}}(x,j)=2\ell^2[K^{\lambda\mu}_{RR}(x,j)+K^{\lambda\mu}_{RL}(x,j)], \quad (20)$$

$$K^{\lambda\mu}_{\Theta}(x,j)=K^{\lambda\mu}_{\mathrm{c}}(x,j)=2\ell^2[K^{\lambda\mu}_{RR}(x,j)-K^{\lambda\mu}_{RL}(x,j)]. \quad (21)$$

Integration over the Φ fields in Eq. (16) yields an effective action in terms of the Θ fields alone,

$$\mathcal{S}_\Theta = \frac{1}{2}\int_{\mathbf{q},\omega}\sum_{\lambda,u}\left[\Theta^{\lambda *}(\mathbf{q},\omega) \times\left(\frac{\omega^2}{\pi^2}(K_\Phi^{-1}(\mathbf{q}))^{\lambda\mu}+q_x^2 K_\Theta^{\lambda\mu}(\mathbf{q})\right)\Theta^u(\mathbf{q},\omega)\right]. \quad (22)$$

The corresponding $\mathcal{S}_\Phi$ action, obtained by integrating out the Θ fields, differs only through the interchange of Φ and Θ and K_Φ, K_Θ.

C. Microscopic theory of long-wavelength interaction parameters

The objective of this coupled-Luttinger-liquid model for stripe states in quantum Hall bilayers is to address the consequences of weak quantum fluctuations when the ground state is similar to the mean-field-theory stripe state. In this spirit, we use weak-coupling expressions for the interaction parameters of the model, replacing scattering amplitudes by the bare values for the scattering of the Hartree-Fock theory quasiparticles. If the true ground state were a smectic, the values of these parameters would be renormalized somewhat by higher-order scattering processes. We expect that it will prove difficult to systematically improve on the estimates given here for the quantum Hall bilayer case because of the absence of a one-body kinetic-energy term in the relevant microscopic Hamiltonian that would enable a systematic perturbative expansion. We emphasize that a quantitative theory of the forward-scattering amplitudes that has a sound microscopic foundation is *necessary* in order to decide on the relevance of the backscattering interactions we have neglected so far and the character of the true ground state. As emphasized by the work of Fradkin, Kivelson, and co-workers,[27] any conclusion is possible if the forward-scattering interactions are allowed to vary arbitrarily. The perturbative renormalization group scaling dimensions that we evaluate below are dependent only on the elastic constants at $q_x=0$, i.e., for straight stripe edges. The weak-fluctuation Hamiltonian may be evaluated in this limit by calculating the expectation value of the microscopic Hamiltonian in the Hartree-Fock theory ground state, which in this limit is a single Slater determinant with straight stripe edges displaced from those in the Hartree-Fock theory stripe ground state. By evaluating the expectation value of the microscopic Hamiltonian in a state with arbitrary stripe edge locations we find that for $j\neq 0$,

$$\int dx K_{\Phi/\Theta}(x,j) = \frac{1}{2\pi^2\ell^2}\begin{pmatrix} V(ja)\mp(ja) & W\mp V(ja-a\nu) \\ W\mp V(ja+a\nu) & V(ja)\mp W(ja)\end{pmatrix}. \quad (23)$$

In the off-diagonal elements the argument of W is the same as that of V, $(ja\pm a\nu)$, respectively. The V and W contributions are proportional to two-particle intralayer and interlayer interaction matrix elements, respectively, and are given by

$$V(Y)=\int\frac{dq}{2\pi}e^{-1/2q^2\ell^2}V_S^N(q)e^{-iqY} - e^{-1/2Y^2/\ell^2}\int\frac{dq}{2\pi}e^{-1/2q^2\ell^2}V_S^N(\sqrt{Y^2/\ell^4+q^2}), \quad (24)$$

$$W(Y)=\int\frac{dq}{2\pi}e^{-1/2q^2\ell^2}V_D^N(q)e^{-iqY}. \quad (25)$$

Note that the intralayer interaction contributions have competing direct and exchange contributions that cancel for $Y=0$, whereas the interlayer interaction has only a direct contribution. In the following we shall assume infinitely narrow quantum wells in both layers so that the interaction potentials occurring in the above equations read

$$V_{S/D}^N(q)=\left[L_N\left(\frac{1}{2}q^2\ell^2\right)\right]^2 V_{S/D}^0(q) \quad , \quad (26)$$

where $L_N(x)$ is the Laguerre polynomial form factor for electrons in the Nth excited Landau-level, and $V_{S/D}^0$ is the Fourier transform of the Coulomb interaction within and between the layers, $V_S^0(q)=e^2 2\pi/|q|$, $V_D^0(q)=e^2(2\pi/|q|)\exp(-|qd|)$ with d being the layer separation. The long-ranged nature of the Coulomb interaction leads to logarithmic divergences in V and W which we regularize by adding a term $-(e^2 2\pi/|q|)\exp(-2|q|d_{\rm gate})$ to $V_{S/D}^0$ with $d_{\rm gate}\gg d$. This regularization can be roughly thought of as introducing a metallic screening plane at distance $d_{\rm gate}$ leading to image charges that screen interactions between electrons in the bilayer system. Although V and W diverge for $d_{\rm gate}\to\infty$, it is possible to show[28] that K_Φ and K_Θ remain finite. In the following we choose a large but finite value for $d_{\rm gate}$ for numerical convenience.

The above form of the smectic energy kernel $K_{\Phi/\Theta}(j)$ applies for $j\neq 0$. For $j=0$ the components of $K_{RL}(0)=K_{LR}(0)$ and of $K_{RR}^{\lambda\mu}(0)=K_{LL}^{\lambda\mu}(0)$ for $\lambda\neq\mu$ are given by the same expressions. The quantities $K_{RR}^{11}(0)=K_{LL}^{11}(0)$ $[=K_{RR}^{22}(0)=K_{LL}^{22}(0)]$ have additional contributions that originate from the wave-vector dependence of the Hartree-Fock self-energy at a given stripe edge, and capture the key property that the energy of the smectic must be invariant under rigid translations of all stripes, $u_{j\alpha}^u(x)\mapsto{}_{j\alpha}^u(x)+\text{constant}$.[19,29] We find that

$$K_{RR}^{11}(0)=-[K_{RR}^{12}(q_y)+K_{RL}^{12}(q_y)+K_{RL}^{11}(q_y)]_{q_y=0} - \sum_{j\neq 0}K_{RR}^{11}(j). \quad (27)$$

Note that these properties imply that $\det[K_\Phi(q_y=0)]=0$. When these long-wavelength approximations are employed, the Fourier transforms of $K_{\Phi/\Theta}^{\lambda u}$ in Eq. (23) depend only on

q_y but not on q_x. From the relation $K_{\Phi/\Theta}(x,-j) = K^T_{\Phi/\Theta}(x,j)$, it follows that $K_{\Phi/\Theta}(q_y)$ is Hermitian. Under particle-hole transformation, $\nu \mapsto 1-\nu$, the diagonal elements of these matrices remain unchanged while the off-diagonal elements transform as

$$K^{12}_{\Phi/\Theta}(q_y) \mapsto e^{-iq_y a} K^{21}_{\Phi/\Theta}(q_y), \tag{28}$$

$$K^{21}_{\Phi/\Theta}(q_y) \mapsto e^{+iq_y a} K^{12}_{\Phi/\Theta}(q_y). \tag{29}$$

D. The balanced bilayer limit

The special case of half filling in each layer has additional symmetry that is most conveniently exploited by taking a slightly different approach. In this case, the electron stripes in both layers have the same width and the system therefore has effective periodicity of $a/2$. To be more precise, the problem can be formulated as a one-dimensional lattice of equidistant double edges placed a distance $a/2$ apart, noting carefully that right and left goers interchange their layer labels on alternate edges. To describe this system instead of using coupling matrices $K^{\lambda u}_{\Phi}(x,j)$ and $K^{\lambda u}_{\Theta}(x,j)$, as in the unbiased case, one can simply use the coupling constants $\tilde{K}_{\Phi}(x,j)$ and $\tilde{K}_{\Theta}(x,j)$,

$$\tilde{K}_{\Phi/\Theta}(x,j) = 2l^2[K_{RR}(x,j) \pm K_{RL}(x,j)] \tag{30}$$

with the value for $K_{RR}(0)$ reflecting translation invariance

$$K_{RR}(0) = -\frac{1}{4\pi^2 l^2} \sum_{j=-\infty}^{+\infty} (-1)^j [V(j) - W(j)]. \tag{31}$$

In momentum space $\tilde{K}_{\Phi}$ and $\tilde{K}_{\Theta}$ have the following form,

$$\tilde{K}_{\Phi}(q_y) = \frac{1}{2\pi^2}\left[V\left(q_y - \frac{2\pi}{a}\right) - V\left(\frac{2\pi}{a}\right) - W\left(q_y - \frac{2\pi}{a}\right) + W\left(\frac{2\pi}{a}\right)\right], \tag{32}$$

$$\tilde{K}_{\Theta}(q_y) = \frac{1}{2\pi^2}\left[V(q_y) - V\left(\frac{2\pi}{a}\right) + W(q_y) + W\left(\frac{2\pi}{a}\right)\right]. \tag{33}$$

We have used this simpler and partially independent formulation of the $\nu = 1/2$ limit, to test our results for the general case.

III. SMECTIC STATE PROPERTIES

A peculiar property of quantum Hall stripe states is that the microscopic scale of backscattering interactions is weak. For this reason observable properties may be those of smectic states over a wide interval of temperature, even when backscattering interactions are relevant at the smectic fixed point. In this section we discuss some characteristic properties of quantum Hall bilayer stripe states.

A. Collective modes and thermodynamic properties

The coupled-Luttinger-liquid model for bilayer quantum Hall stripe states gives rise to two collective modes with dispersions that can be determined by evaluating zeros of the determinant of the 2×2 matrix that defines the real-time quadratic action at each $\mathbf{q}$ and ω. Writing this matrix (with indices suppressed) as $K_{\Phi}^{-1}[\omega^2 + \pi^2 q_x^2 K_{\Phi} K_{\Theta}]/\pi^2$, it follows that the squares of the quadratic boson collective mode energies are

$$\omega^2_{\pm}(\mathbf{q}) = v^2_{\pm}(\mathbf{q}) q_x^2 = \pi^2 q_x^2 \frac{\mathrm{Tr}[K_{\Phi}(\mathbf{q}) K_{\Theta}(\mathbf{q})]}{2} \times \left[1 \pm \sqrt{1 - \frac{4\det[K_{\Phi}(\mathbf{q}) K_{\Theta}(\mathbf{q})]}{\mathrm{Tr}^2[K_{\Phi}(\mathbf{q}) K_{\Theta}(\mathbf{q})]}}\right]. \tag{34}$$

Both modes have energies that are proportional to q_x. The velocity of the $\omega_-(\mathbf{q})$ mode vanishes for $q_y \to 0$. In fact, when the q_x dependence of K_{Φ} and K_{Θ} is dropped, as in most of our calculations $\omega_-(q_x, q_y = 0)$ vanishes identically; when the q_x dependences are restored $\omega^2_-(\mathbf{q}) \approx q_x^2(q_y^2 + q_x^4)$ at small wave vectors and $\omega_-(q_x, q_y = 0) \propto q_x^3$. For gate-screened Coulomb interactions, the x-direction ω_- mode velocity is proportional to $|q_y|$ in the small q_x and q_y limit. In the independent layer limit, the two modes become degenerate and we recover the isolated layer results obtained previously.[19]

In the case of balanced bilayers the alternate formulation mentioned above is more convenient. The collective modes for this limit may be expressed as

$$\omega_{1,2}(\mathbf{q}) = \pi q_x \sqrt{\tilde{K}_{\Phi}(\mathbf{q}) \tilde{K}_{\Theta}(\mathbf{q})}, \tag{35}$$

where $\tilde{K}_{\Phi}(\mathbf{q})$ and $\tilde{K}_{\Theta}(\mathbf{q})$ are given by Eqs. (32) and (33). The two collective modes of the general formulation applied to the $\nu = 1/2$ case correspond to two different wave vectors of this dispersion relation.

The collective modes of the bilayer Quantum Hall smectic phase are shown in Fig. 2. The right panel shows $\omega_+(q_x, q_y)$ that disperses linearly in small q_x for arbitrary q_y. In contrast, $\omega_-(q_x, q_y)$ disperses linearly at small q_x for $q_y \neq 0$, but for $q_y = 0$ it is sublinear: $\omega_-(q_x, q_y = 0) \sim q_x^3$.

The thermodynamic properties of the smectic phase of the bilayer system are those of a noninteracting boson system and are readily evaluated given the collective mode energies. For example, for $\nu = 1/2$ in each layer, using the simpler alternative formulation, we have one collective mode at each wave vector. The internal energy density is

$$U = \int \frac{d^2q}{(2\pi)^2/a} \frac{\omega(\mathbf{q})}{e^{\omega(\mathbf{q})/T} - 1}, \tag{36}$$

where $\omega(\mathbf{q})$ is given by Eq. (35). At low temperatures only the long-wavelength behavior matters and we obtain

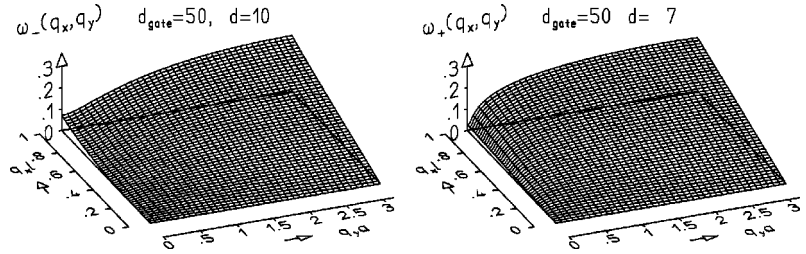

FIG. 2. Collective modes of the bilayer QH smectic phase. These results shown here were evaluated using $K_{\Phi/\Theta}(x,j)$ values from Eqs. (23)–(25) with $N=2$, $\nu\approx 1/2$, and $a=5.8l$. Notice that $\omega_+(q_x,q_y)$ always disperses linearly for small q_x, whereas $\omega_-(q_x,q_y)$ disperses sublinearly (as q_x^3) when $q_y=0$. The $q_y=0$ behavior of the lower collective mode is sensitive to the q_x dependence of the interaction coefficients which we do not evaluate microscopically. This illustration was constructed by adding a small q_x^4 contribution to the interaction coefficients.

$$U\approx \int \frac{dq_x dq_y}{(2\pi)^2/a}\frac{\pi|q_x||q_y|\sqrt{\tilde{K}_\Theta(0)\tilde{K}''_\Phi(0)}}{e^{\pi|q_x||q_y|\sqrt{\tilde{K}_\Theta(0)\tilde{K}''_\Phi(0)}/T}-1}$$

$$=\frac{2a}{\pi^3\sqrt{\tilde{K}_\Theta(0)\tilde{K}''_\Phi(0)}}T^2\zeta(2)\ln\left(\frac{T_0}{T}\right), \tag{37}$$

where $k_BT_0=\sqrt{\tilde{K}_\Theta(0)\tilde{K}''_\Phi(0)}/al$. The specific heat of this system varies as $T\ln(T_0/T)$ at small T, vanishing less quickly than that of a noninteracting Fermion system because of the soft collective modes that result from the translational invariance of the stripe state. This low temperature behavior reflects the form of the dispersion relation at small $\mathbf{q}$, $\omega_-(\mathbf{q})\sim q_xq_y$; only the prefactor of this enhanced specific heat changes in the unbalanced bilayer case. These results for the specific heat are similar to that obtained in previous works by Barci *et al.*,[24] and Lopatnikova *et al.*[23] for the case of a single layer. There is no qualitative difference between the thermodynamic properties of single-layer and bilayer stripe states. For unbalanced bilayers the specific heat at low temperatures is dominated by the softer of the two collective modes, whose long-wavelength dispersion is given by

$$\omega_-(\mathbf{q})\approx q_xq_y\sqrt{\frac{\mathrm{Tr}[K_\Phi(0)K_\Theta(0)]}{\det[K_\Theta(0)][\det(K_\Phi)]''(0)}}. \tag{38}$$

It follows that the internal energy is given by

$$U\approx\frac{a}{\pi^3}\sqrt{\frac{\mathrm{Tr}[K_\Phi(0)K_\Theta(0)]}{\det[K_\Theta(0)][\det(K_\Phi)]''(0)}}T^2\zeta(2)\ln\left(\frac{T_0}{T}\right), \tag{39}$$

and the specific heat will vary again as $T\ln(T_0/T)$. The T_0 in Eqs. (39) and (37) are given by corresponding expressions.

B. Boson and fermion correlation functions at the smectic fixed point

In this section we discuss the static and dynamic correlation functions of the right- and left-moving fermions of the stripe edges and the boson correlation functions in terms of which they are evaluated. The right- and left-moving fermion fields are expressed in terms of the Φ and Θ boson fields as follows:

$$R_j^\lambda(x,\tau)=\frac{1}{\sqrt{2\pi}}e^{i\phi^\lambda_{j,R}(x,\tau)}=\frac{1}{\sqrt{2\pi}}e^{i[\Phi_j^\lambda(x,\tau)+\Theta_j^\lambda(x,\tau)]}, \tag{40}$$

$$L_j^\lambda(x,\tau)=\frac{1}{\sqrt{2\pi}}e^{i\phi^\lambda_{j,L}(x,\tau)}=\frac{1}{\sqrt{2\pi}}e^{i[\Phi_j^\lambda(x,\tau)-\Theta_j^\lambda(x,\tau)]}, \tag{41}$$

where the Φ field is related to position fluctuations of the two-edge system, while the Θ field is related to its charge-density fluctuations. We observe in the following that the charge and position fluctuations of the edges have a dramatically different effect on the correlation functions of the right and left movers. The single-particle Green's function for the right movers is given by

$$\langle R_j^{\lambda\dagger}(x,\tau)R_j^\lambda(0,0)\rangle=\frac{1}{2\pi}e^{-1/2\langle[\Phi_j^\lambda(x,\tau)-\Phi_j^\lambda(0,0)]^2\rangle}\times e^{-1/2\langle[\Theta_j^\lambda(x,\tau)-\Theta_j^\lambda(0,0)]^2\rangle}. \tag{42}$$

We first evaluate the Φ and Θ field correlation functions $\tilde{C}_\Phi^{\lambda\lambda}$ and $\tilde{C}_\Theta^{\lambda\lambda}$, where

$$\tilde{C}_\Phi^{\lambda\lambda}(x,0,0)=\langle[\Phi_j^\lambda(x,\tau)-\Phi_j^\lambda(0,\tau)]^2\rangle, \tag{43}$$

and similarly for $\tilde{C}_\Theta^{\lambda\lambda}$. In Eq. (43) and in the following the arguments of $\tilde{C}_{\Phi/\Theta}^{\lambda\lambda}$ are $(x-x',j-j',\tau-\tau')$. From Eq. (22) we have for the Φ_j^λ field

$$\tilde{C}_\Phi^{\lambda\lambda}(x,0,0)=2\int\frac{d^2qd\omega}{(2\pi)^3/a}[1-\cos(q_xx)][M_\Phi^{-1}(\mathbf{q},\omega)]^{\lambda\lambda}, \tag{44}$$

where

$$M_\Phi^{\lambda u}(\mathbf{q},\omega)=\frac{\omega^2}{\pi^2}[K_\Theta^{-1}(q_y)]^{\lambda u}+q_x^2[K_\Phi(q_y)]^{\lambda u}. \tag{45}$$

$M_\Theta(\mathbf{q},\omega)$ can be obtained by interchanging K_Φ, K_Θ. The integral over ω is readily valued by decomposing M_Φ^{-1} as a sum over eigenmode contributions, writing it in the form $\Sigma_\pm C_\pm^{\lambda u}/[\omega^2+\omega_\pm^2(\mathbf{q})]$. It follows after some algebra that correlation function can be expressed in the form

$$\tilde{C}^{\lambda\lambda}_{\Phi}(x,0,0) = \int_0^{\Lambda} dq_x \frac{[1-\cos(q_x x)]}{q_x} \int_{-\pi/a}^{\pi/a} \frac{dq_y}{2\pi/a} \times \left[\frac{\det(K_\Theta)}{K_+ + K_-} \left((K_\Theta^{-1})^{\lambda\lambda} + \frac{K_\Phi^{\lambda\lambda}}{K_+ K_-} \right) \right] \approx \ln\left(\frac{|x|}{l} \right) \int \frac{dq_y}{2\pi/a} \left[\frac{\det(K_\Theta)}{K_+ + K_-} \left((K_\Theta^{-1})^{\lambda\lambda} + \frac{K_\Phi^{\lambda\lambda}}{K_+ K_-} \right) \right], \tag{46}$$

for large x, where $K_\pm = v_\pm(\mathbf{q})/\pi$. In the limit of balanced filling fraction for which K_Φ and K_Θ are scalars, the integrand which is averaged over q_y above reduces to $\sqrt{\tilde{K}_\Theta/\tilde{K}_\Phi}$, the familiar result for Φ-field correlation functions in a standard one-dimensional electron system. This result is generalized here by the average over q_y and by the particular way, in which the matrix nature of the K_Θ and K_Φ expressions enter the matrix elements above. The result for the Θ-field correlation functions differs only by the interchange of the K_Θ and K_Φ matrices. At first sight it appears that the position fluctuation factor in the right-mover correlation function decays algebraically along the stripes. However, the power which characterizes this decay, $d_{\Phi,x}$, is given by the integral over q_y of Eq (46), which diverges logarithmically, because $K_- \propto v_-$ vanishes as $|q_y|$ as $|q_y| \to 0$; the same soft position fluctuations that led above to an enhanced specific heat, lead here to fermion correlation functions that decay faster than any power low but slower than an exponential. This observation generalizes to bilayers, a property of single-layer stripe states noted by Lopatnikova *et al.*[23] and Barci *et al.*[24]

$\tilde{C}_\Theta(x,0,0)$, which specifies the charge fluctuation factor in the fermion correlation functions, is given by

$$\tilde{C}^{\lambda\lambda}_{\Theta}(x,0,0) \approx \ln\left(\frac{|x|}{l} \right) \int_{-\pi/a}^{\pi/a} \frac{dq_y}{2\pi/a} \times \left[\frac{\det(K_\Phi)}{K_+ + K_-} \left((K_\Phi^{-1})^{\lambda\lambda} + \frac{K_\Theta^{\lambda\lambda}}{K_+ K_-} \right) \right]. \tag{47}$$

The charge fluctuation factor in the fermion correlation functions has a conventional algebraic decay with finite power $d_{\Theta,x}$. The faster than algebraic decay of the fermion one-particle Green's function implies that the singularity in the Landau gauge occupation numbers, a step function of unit magnitude in the Hartree-Fock theory, is exceedingly weak.

The correlation function of the Φ field along directions perpendicular to the stripes is given by

$$\tilde{C}^{\lambda\lambda}_{\Phi}(0,y,0) \approx \int_{1/L}^{\Lambda} \frac{dq_x}{q_x} \int_{-\pi/a}^{\pi/a} \frac{dq_y}{2\pi/a} [1-\cos(q_y y)] \times \left[\frac{\det(K_\Theta)}{K_+ + K_-} \left((K_\Theta^{-1})^{\lambda\lambda} + \frac{K_\Phi^{\lambda\lambda}}{K_+ K_-} \right) \right] \approx C \ln\left(\frac{L}{l} \right) \ln\left(\frac{|y|}{a} \right), \tag{48}$$

where C is a finite constant that can be found numerically. It follows that the corresponding factor in the one-particle Green's function has a faster than algebraic decay in the thermodynamic limit. The factor associated with charge fluctuations has a similar dependence and is given by

$$C^{\lambda\lambda}_{\Theta}(0,y,0) \approx \int_{1/L}^{\Lambda} \frac{dq_x}{q_x} \int_{-\pi/a}^{\pi/a} \frac{dq_y}{\frac{2\pi}{a}} \cos(q_y y) \times \left[\frac{\det(K_\Phi)}{K_+ + K_-} \left((K_\Phi^{-1})^{\lambda\lambda} + \frac{K_\Theta^{\lambda\lambda}}{K_+ K_-} \right) \right] \approx \ln\left(\frac{L}{l} \right) C_\Theta\left(\frac{a}{|y|} \right), \tag{49}$$

where C_Θ is a function of the ratio $(a/|y|)$ and is finite as $|y| \to +\infty$.

C. Tunneling density of states

These results for boson correlation functions may be assembled to evaluate the imaginary time dependence of the local fermion Matsubara Green's function and, by Laplace transforming this, the density of states for tunneling into the bilayer system, a quantity that is in principle measurable. The single-particle Matsubara Green's function is given by

$$G(0,0,\tau) = \langle R_j^{\lambda\dagger}(x,\tau) R_j^{\lambda}(x,0) \rangle \approx \exp\{-(1/2)\tilde{C}(\tau)\}, \tag{50}$$

where $\tilde{C}(0,0,\tau) = \tilde{C}_\Phi(0,0,\tau) + \tilde{C}_\Theta(0,0,\tau)$ and

$$\tilde{C}_{\Phi/\Theta}(0,0,\tau) = 2 \int \frac{d^2q\, d\omega}{(2\pi)^3/a} (1-\cos\omega\tau) [M^{-1}_{\Phi/\Theta}(\mathbf{q},\omega)]^{\lambda\lambda}. \tag{51}$$

We first discuss the balanced bilayer case for which the $K_\Phi^{\lambda u}$ and $K_\Theta^{\lambda u}$ matrices become simple numbers and the integral is simpler to treat analytically. In this case $\tilde{K}_\Phi(q_y)$, $\tilde{K}_\Theta(q_y)$, are given by Eqs. (32)–(33) and

$$\tilde{C}_\Phi(0,0,\tau) = 2 \int \frac{d^2q\, d\omega}{(2\pi)^3/a} \frac{(1-\cos\omega\tau)}{\frac{\omega^2}{\pi^2 \tilde{K}_\Theta(q_y)} + \tilde{K}_\Phi(q_y) q_x^2} = \int \frac{d^2q}{4\pi/a} \frac{1}{|q_x|} \sqrt{\frac{\tilde{K}_\Theta(q_y)}{\tilde{K}_\Phi(q_y)}} \times (1 - e^{-\pi|q_x|\sqrt{\tilde{K}_\Phi(q_y)\tilde{K}_\Theta(q_y)}\,\tau}). \tag{52}$$

We can understand the content of this integral by means of the following analysis. The integral can be separated into the sum of two terms, contributions from the region where q_x and q_y are small and the exponential can be approximated by the first few terms of the Taylor expansion, and contributions from larger q_x and q_y where the exponential can be disregarded. The leading contribution to the integral comes form the lower boundary of the second region, where q_y

$\approx 1/(q_x\tau)$. We focus on the case of large τ for which our low-energy theory applies. In this limit we can approximate $\tilde{K}_\Theta(q_y)\approx\tilde{K}_\Theta(0)$ and $\tilde{K}_\Phi(q_y)\approx\tilde{K}''_\Phi(0)q_y^2$. In this limit Eq. (52) becomes

$$\tilde{C}_\Phi(0,0,\tau)=\frac{a}{4\pi}\sqrt{\frac{\tilde{K}_\Theta(0)}{\tilde{K}''_\Phi(0)}}\int\frac{dq_x dq_y}{|q_x||q_y|}\times(1-e^{-\pi|q_x||q_y|\tau\sqrt{\tilde{K}_\Theta(0)\tilde{K}''_\Phi(0)}})\approx\frac{a}{2\pi}\sqrt{\frac{\tilde{K}_\Theta(0)}{\tilde{K}''_\Phi(0)}}\ln^2\left(\frac{\pi^3}{al}\sqrt{\tilde{K}_\Theta(0)\tilde{K}''_\Phi(0)}\tau\right). \tag{53}$$

The Matsubara Green's function factor contributed by Θ-field correlations has a weaker τ dependence which we can neglect for the present qualitative analysis.

Similar steps can be taken for the general case of unbalanced bilayers. After the ω integration, for Eq. (51) we obtain

$$\tilde{C}_\Phi(0,0,\tau)=\frac{a}{4\pi}\int\frac{d^2q}{|q_x|}\frac{K^{11}_\Theta}{K_+^2-K_-^2}\left\{\left[\left(K_+-\frac{K^{22}_\Phi}{(K_\Theta^{-1})^{22}}\frac{1}{K_+}\right)-\left(K_--\frac{K^{22}_\Phi}{(K_\Theta^{-1})^{22}}\frac{1}{K_-}\right)\right]-\frac{1}{K_+^2-K_-^2}\left[\left(K_+-\frac{K^{22}_\Phi}{(K_\Theta^{-1})^{22}}\frac{1}{K_+}\right)e^{-\omega_+(q_y)\tau}-\left(K_--\frac{K^{22}_\Phi}{(K_\Theta^{-1})^{22}}\frac{1}{K_-}\right)e^{-\omega_-(q_y)\tau}\right]\right\}. \tag{54}$$

Since at small q_y, $K_-\sim|q_y|$, the most important contributions to the integral will come from the terms containing $1/K_-$ and from the exponential factors containing the argument $\omega_-(q_y)$. Keeping only these terms we obtain

$$\tilde{C}_\Phi(0,0,\tau)\approx\frac{a}{4\pi}\frac{K^{11}_\Theta(0)}{K_+^2(0)K''_-(0)}\frac{K^{22}_\Phi(0)}{(K_\Theta^{-1})^{22}(0)}\int\frac{dq_x dq_y}{|q_x||q_y|}\times\left(1-\frac{1}{K_+^2(0)}e^{-\pi K''_-(0)\tau|q_x||q_y|}\right)\approx\frac{a}{2\pi}\frac{\det(K_\Theta)(0)}{K_+^2(0)K''_-(0)}K^{22}_\Phi(0)\ln^2\left(\frac{\pi^3}{al}K''_-(0)\tau\right), \tag{55}$$

demonstrating that the form of the Matsubara Green's function does not change qualitatively at unbalanced filling factors. The tunneling density of states is the inverse Laplace transform of $G(0,0,\tau)$,

$$G(0,0,\tau)\approx e^{-(\alpha/2)\ln^2(\Omega_0\tau)}=\int_0^{+\infty}dE\,\rho_{\rm Tunn}(E)e^{-E|\tau|}, \tag{56}$$

where α and Ω_0 can be identified from Eq. (54) for balanced bilayers and from Eq. (56) in the unbalanced case. The inverse Laplace transform of such a function is

$$\rho_{\rm Tunn}(E)=\frac{e^{-(\alpha/2)\ln^2(\Omega_0/E)}}{E/\Omega_0}\sum_{k=0}^{\infty}\frac{\Gamma_k(1)}{k!}\times\left(-\frac{\sqrt{\alpha}}{\sqrt{2}}\right)^{k+1}H_{k+1}\left[\frac{\sqrt{\alpha}}{\sqrt{2}}\ln\frac{E}{\Omega_0}\right], \tag{57}$$

where $\Gamma_k(1)$ is the kth derivative of $1/\Gamma(r)$ at $r=1$ and H_k are the Hermite polynomials. In the asymptotic case of small E (low energies), we have

$$\rho_{\rm Tunn}(E)\sim\frac{e^{-(\alpha/2)\ln^2(\Omega_0/E)}}{E/\Omega_0}\frac{\alpha\ln(\Omega_0/E)}{\Gamma(1+\alpha\ln(\Omega_0/E))}\approx\exp\left\{-\frac{\alpha}{2}\ln^2\frac{\Omega_0}{E}-\left(\alpha\ln\frac{\Omega_0}{E}-\frac{1}{2}\right)\ln\ln\frac{\Omega_0}{E}+\ln\frac{\Omega_0}{E}\right\}. \tag{58}$$

This shows that the density of states vanishes at the Fermi energy stronger than any power of E and that in this sense the stripe edge physics in bilayer quantum Hall systems is not that of a usual system of weakly-coupled Luttinger-liquids. The above result generalizes to the case of bilayer systems, points that have been made about single-layer quantum Hall stripe states by Lopatnikova *et al*[23] and Barci *et al*.[24]

IV. STABILITY OF THE QUANTUM HALL SMECTIC PHASE

We now consider "backward" (interchannel) scattering interactions that do not conserve the number of electrons in each stripe edge. The most important conclusion of the following analysis is that backscattering interactions are much more important for bilayer stripe states than for single-layer stripe states. We can classify the backscattering interactions as either intralayer interactions that involve electrons only in one layer or interlayer interactions that involve electrons in both layers. Nonzero backscattering two-particle matrix elements conserve total momentum along the stripes, which means that the two Landau gauge guiding center jumps must sum to zero. In the case of quantum Hall stripe states, the microcopic matrix elements associated with these backscattering processes tend to be small and these interactions will be important only if they produce strong infrared divergences in perturbation theory. The strength of these divergences is characterized here by evaluating lowest-order perturbative renormalization group scaling dimensions for these operators. As in Ref. 19 our renormalization group (RG) scheme involves only x and τ dimensions and treats the rung label as an internal index of the fields Φ_j^λ, Θ_j^λ. The philosophy underlying this procedure is discussed in the following section.

A. Interlayer tunneling

We first address the tunneling of an electron from one stripe edge to the other in the same rung. The action contribution from this process has the following bosonized form:

$$\mathcal{S}_{\rm Tunn} = -u \int dx d\tau \sum_j \sum_\lambda [\exp(i2\Theta_j^\lambda) + \text{H.c.}], \quad (59)$$

where the microscopic amplitude u is discussed below. We integrate out "fast" boson modes Φ^λ, Θ^λ in a shell, with $\Lambda/b < |q_x| < \Lambda$ and ω, q_y unrestricted, and then rescale $q_x' = bq_x$ and $\omega' = b\omega$ leaving q_y unchanged. With an appropriate rescaling of Φ, this RG transformation leaves the harmonic smectic action S_0 [and dispersion relation (34) for $K_{\Phi/\Theta}$ (23)], invariant. Stability of the smectic fixed point in the presence of backscattering can be tested by considering the lowest-order RG flow equation,

$$\frac{\partial u}{\partial t} = (2 - \Delta_{\rm Tunn})u, \quad (60)$$

with $t = \ln b$. As can be seen from this equation the tunneling operator will become relevant when its scaling dimension is less than two. When this term in the Hamiltonian is strong, the system is described at low energies by a set of quantum sine-Gordon models coupled by gradient terms (22). In the domain $0 < \Delta_{\rm Tunn} < 2$ the continuous symmetry, present in Eq. (22), and broken by tunneling, is lost in the low-energy fixed point action. This model has a discrete symmetry $\Theta_j^\lambda \to \Theta_j^\lambda + \pi n$ for any integer n and the QFT becomes massive.[30] The gap due to tunneling will lead to an integer quantum Hall effect at total filling factor $\nu_T = 1$. Using Eqs. (22), and (59), we find the following expression for the scaling dimension

$$\Delta_{\rm Tunn} = \int_{-\pi/a}^{\pi/a} \frac{dq_y}{\frac{2\pi}{a}} \left[\frac{\det K_\Phi}{K_+ + K_-} \left((K_\Phi^{-1})^{11} + \frac{K_\Theta^{11}}{K_+ K_-} \right) \right]. \quad (61)$$

The integrand in the integral over q_y is similar to that involved in the Θ boson correlation field and, ignoring the matrix character of the coefficients that appear in the smectic fixed point Hamiltonian, is $\sim \sqrt{K_\Phi / K_\Theta}$. Since K_Φ vanishes for $q_y \to 0$, we can expect this quantity to be small. Indeed we find by evaluating this integral numerically that interlayer tunneling is always relevant.

B. Coulomb backscattering interactions

The tunneling amplitude in bilayer quantum Hall systems can be made extremely small by making the barrier between quantum wells higher or wider and is often completely negligible in practice. Coulomb interactions, on the other hand, are always present and must always be considered. We consider *interlayer* and *intralayer* Coulomb backscattering processes separately. In the strongest interlayer backscattering process an electron is transferred from, say, a left-moving top layer stripe edge to a right-moving edge in the same rung pair of the same layer, while in the same rung pair of the bottom layer an electron is transferred in the opposite direction, as depicted in Fig. 1. The interlayer backscattering operators for processes involving neighboring rungs have large scaling dimensions and tend to be irrelevant. In addition, the bare matrix elements for such a process will fall off rapidly in magnitude with increasing distance between the rungs involved. The action for interlayer backscattering interactions for electrons within the same rung pair reads

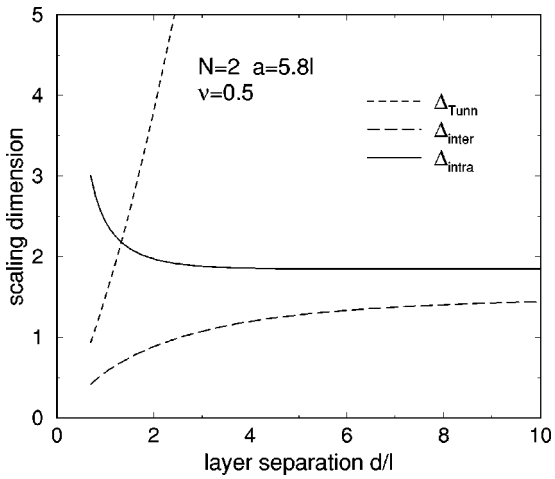

FIG. 3. Scaling dimensions for tunneling and backscattering interactions as a function of layer separation d/l in a balanced bilayer system at bilayer total filling factor $\nu_T = 9$, i.e., with a $N = 2$ valence Landau-level.

$$\mathcal{S}_{\rm inter} = -u \int dx d\tau \sum_j [\exp(i2(\Theta_j^1 + \Theta_j^2)) + \text{H.c.}]. \quad (62)$$

[The other kind of process involving two neighboring rung pairs is related to the above one by a particle-hole transformation $\nu \mapsto 1 - \nu$].

After an elementary calculation we obtain the following scaling dimension expression:

$$\Delta_{\rm inter} = \int_{-\pi/a}^{\pi/a} \frac{dq_y}{\frac{2\pi}{a}} \left[\frac{2 \det K_\Phi}{K_+ + K_-} \times \left((K_\Phi^{-1})^{11} - (K_\Phi^{-1})^{12} + \frac{K_\Theta^{11} - K_\Theta^{12}}{K_+ K_-} \right) \right]. \quad (63)$$

This expression is similar to that which would be obtained for interwire backscattering interactions in a systems of two coupled quantum wires. This integral is similar to the one that appears in the tunneling operator scaling dimension calculation, although it is easy to verify that forward-scattering interactions between different stripes play an essential role. As we discuss below, this operator is usually strongly relevant ($\Delta_{\rm inter} \to 0$), so that at low temperatures the phases Θ_j^1 and Θ_j^2 of neighboring two-edge system are strongly anticorrelated. The low-energy nontopological (chargeless) excitations in this limit can be understood by approximating $\cos[(\Theta_j^1 + \Theta_j^2)] \approx 1 - (\Theta_j^1 + \Theta_j^2)^2/2$. When a term of this form is

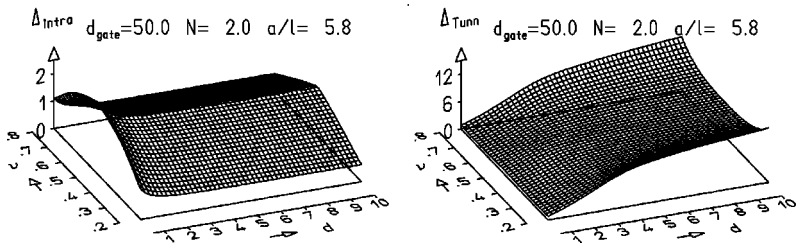

FIG. 4. The left panel shows the $N=2$, $d/\ell=5.8$, intralayer backscattering interaction scaling dimension. The right panel shows the scaling dimension of the tunneling operator.

added to the quadratic Hamiltonian, the low-energy collective mode dispersion at long wave lengths takes the form of a spatially anisotropic two-dimensional XY ferromagnet, $\omega^2 \sim K q_x^2 + u q_y^2$. We discuss the significance of this result at greater length below.

Finally, in an intralayer backscattering process two electrons move in opposite directions between pairs of stripe edges in the same layer with the same separation (cf. Fig 1). Here we also concentrate on processes involving neighboring rungs only. Processes involving two rung pairs are again related to those involving three pairs by a particle-hole transformation. For the first case the action reads

$$\mathcal{S}_{\rm intra} = -u \int dx d\tau \sum_j \{\exp[i(\Phi_j^2 - \Phi_j^1 + \Phi_{j+1}^1 - \Phi_{j+1}^2)] \times \exp[i(-\Theta_j^2 - \Theta_j^1 + \Theta_{j+1}^1 + \Theta_{j+1}^2)] + \text{H.c.}\}, \quad (64)$$

which leads to a scaling dimension $\Delta_{\rm intra} = \Delta_\Phi + \Delta_\Theta$ with

$$\Delta_\Phi = \int_{-\pi/a}^{\pi/a} \frac{dq_y}{\frac{2\pi}{a}} \frac{\det K_\Theta}{K_+ + K_-} [1 - \cos(q_y a)] \times \left((K_\Theta^{-1})^{11} + (K_\Theta^{-1})^{12} + \frac{K_\Phi^{11} + K_\Phi^{12}}{K_+ K_-} \right), \quad (65)$$

$$\Delta_\Theta = \int_{-\pi/a}^{\pi/a} \frac{dq_y}{\frac{2\pi}{a}} \frac{\det K_\Phi}{K_+ + K_-} [1 - \cos(q_y a)] \times \left((K_\Phi^{-1})^{11} - (K_\Phi^{-1})^{12} + \frac{K_\Theta^{11} - K_\Theta^{12}}{K_+ K_-} \right). \quad (66)$$

Note that the imaginary part of the integrand in Eqs. (63), (65) and (66) does not contribute to the integrals. Backscattering processes other than those discussed above have larger scaling dimensions and also involve larger momentum transfer, and have therefore exponentially smaller bare matrix elements. We therefore shall concentrate on the processes discussed above.

We now discuss our numerical results for scaling dimensions of the operators that are not described by the quadratic boson theory. Figure 3 shows the scaling dimensions of the backscattering interactions in a balanced system ($\nu=1/2$) in the second-excited Landau-level ($N=2$) as a function of the layer separation d/ℓ. The stripe period chosen for these calculations, $a=5.8\ell$, corresponds to the period at which the Hartree-Fock energy of the stripe state in a isolated layer is minimized.[31] Interestingly, single-electron tunneling is irrelevant ($\Delta_{\rm Tunn}>2$) for $d/\ell>1.5$, but is strongly relevant at smaller layer separations. Interlayer backscattering is relevant ($\Delta_{\rm inter}<2$) at all layer separations, more strongly so at smaller layer separations, while the scaling dimension of the intralayer backscattering is smaller than two only for $d/\ell \gtrsim 2$ and approaches a value of $\Delta_{\rm intra} \approx 1.84$ for $d/\ell \gg 1$. This value for the limit of weak interactions between the layers recovers the single-layer result obtained earlier.[19] The contributions Δ_Φ and Δ_Θ to $\Delta_{\rm intra}$, not shown in the figure, become equal in this case.

The dependence of scaling dimensions on the bilayer balance is illustrated in Figs. 4 and 5. We see that intralayer interactions become more relevant when their individual filling factors move away from $\nu=0.5$, as in the single-layer case, while the tunneling operator becomes less relevant. Interestingly, the interlayer backscattering interactions show different results depending on the distance between the edges involved in the transition. For $\nu \neq 0.5$ we have to distinguish between nearest-neighbor interlayer and intralayer backscattering processes that involve, according to the definition given in Fig. 1, only the smallest number of neighboring rung pairs (one and two, respectively) and those processes that involve formally two and three rung pairs, respectively. These two kinds of processes are related by particle-hole transformation, and therefore shown in different panels. Generally the scaling dimension increases with the distance between the edges. The data shows that one of these two backscattering processes, related by a particle-hole transformation, is always relevant and that the minimum scaling dimension decreases with increasing bias between the layers. In summary, the most relevant residual interac-

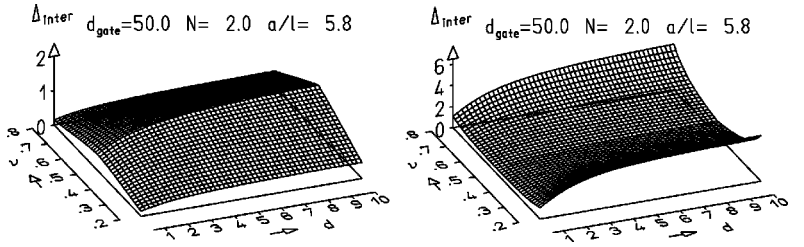

FIG. 5. The left panel shows the scaling dimensions for interlayer backscattering across narrow and the right panel for interlayer backscattering across wide rungs in unbalanced bilayers. Note the difference in scale between left and right panels. The most relevant interlayer backscattering interactions are those of narrow rungs.

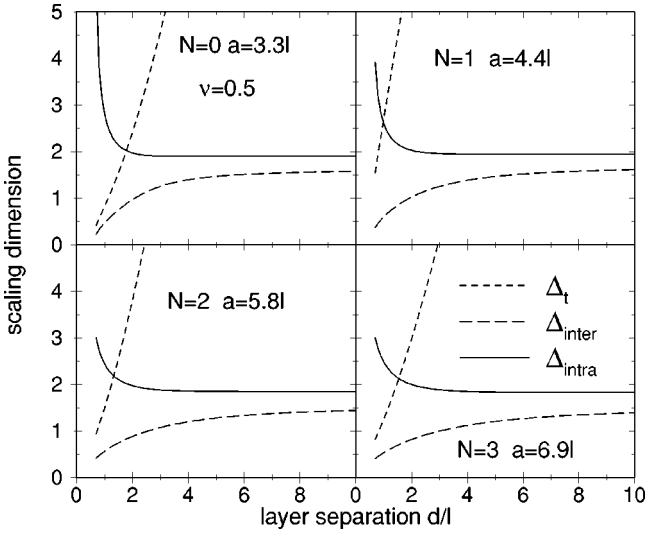

FIG. 6. The scaling dimension of the backscattering interactions in the various Landau-level ($N=0,1,2,3$) in a balanced system as a function of the layer separation d/ℓ. The stripe periods a are obtained from the Hartree-Fock monolayer results given in Ref. 31.

tions is interlayer backscattering and they are increasingly important as the bilayer is unbalanced.

We note that the scaling dimensions Δ_{Tunn} of the single-electron tunneling and Δ_{inter} of the interlayer backscattering approach zero for $d/\ell \to 0$, i.e., these processes become strongly relevant. This is a natural result since in this limit we recover the monolayer electron-spin quantum Hall ferromagnet. This system is perfectly isotropic in pseudospin space, and therefore processes like tunneling which acts essentially like a (pseudo-)magnetic field are obviously very relevant. This increased relevance arises formally in our calculations through the property that the matrices $K_\Phi(q_y)$ vanish in the limit $d \to 0$, so that the integrands in Eqs. (61) and (63) are identically zero. K_Φ vanishes, because it is a measure of energy changes associated with charge transfer between layers at a particular stripe edge; when $d \to 0$ only the total charge near each stripe edge influences the energy functional. In Fig. 6 we show the dependence of these scaling dimensions on the Landau-level index $N=0,1,2,3$ with the stripe periods taken from Ref. 31 in each case. As this figure shows, our results for the scaling dimensions of backscattering processes around the assumed stripe state depend only weakly on the Landau-level index. We note that in the lowest and first-excited Landau-level ($N=0,1$) no conductance anisotropies are found experimentally in single layers, even though there is a stripe state in each of these Landau levels which is a local minimum of the Hartree-Fock energy functional. The true ground state in these instances is far from the stripe state, differencing in character even at microscopic length scales. The fact that our calculation does not obtain anomalous results in cases where we do not believe stripe states occur, emphasizes again that our approach can only address the properties of systems in which fluctuations around the Hartree-Fock stripe states are weak. It cannot predict when stripe states occur. Future experimental activity will be necessary to identify with confidence when stripe states occur in bilayers.

C. Smectic interlayer phase coherent and the Wigner crystal states

1. Smectic interlayer phase-coherent state

In this section we examine the effect of the interlayer backscattering interactions (when they are strongly relevant) on the low-energy physics of the system and show that the phase coherence is marked by a nonvanishing value of an interlayer phase order parameter. In this phase electrons at each stripe edge are coherent superpositions of the upper and lower layer states.

The most relevant interlayer backscattering operators are related by particle-hole symmetry and describe backscattering across an electron stripe in the top layer and the corresponding hole stripe in the bottom layer or across a hole stripe in the top layer and the corresponding electron stripe in the bottom layer. In terms of the Luttinger-liquid fields we have defined, the sum of these two interactions takes the form

$$\hat{O}_{\text{inter}} = -u_{\text{inter},\nu}\cos[2(\Theta_j^1+\Theta_j^2)] - u_{\text{inter},(1-\nu)}\cos[2(\Theta_j^2+\Theta_{j+1}^1)]. \quad (67)$$

Expressions for the bare values of these coupling constants are given below. As shown on Figs. 5(a) and 5(b), (left, right panel, respectively), at small layer separations these operators are strongly relevant. At low temperatures the phases Θ_j^1 and Θ_j^2, Θ_j^2 and Θ_{j+1}^1 of neighboring two edges tend to be strongly anticorrelated. The low-energy excitations in this limit can be understood by approximating $\cos[(\Theta_j^1+\Theta_j^2)] \approx 1 - (\Theta_j^1+\Theta_j^2)^2/2$. When terms of this form are added to the action, it takes the following form:

$$\mathcal{S}_\Theta = \frac{1}{2}\int_{\mathbf{q},\omega}\sum_{\lambda,u}[\Theta^{\lambda *}(\mathbf{q},\omega)\mathcal{M}_\Theta^{\lambda u}\Theta^u(\mathbf{q},\omega)]. \quad (68)$$

The new matrix $\mathcal{M}_\Theta$ is given by

$$\mathcal{M}_\Theta = M_\Theta + 2\begin{pmatrix} u_{i1}+u_{i2} & u_{i1}+u_{i2}e^{-iq_y a} \\ u_{i1}+u_{i2}e^{iq_y a} & u_{i1}+u_{i2} \end{pmatrix}, \quad (69)$$

where M_Θ is the matrix of the system at the smectic fixed point and is given by Eq. (22) or by Eq. (45) (interchanging K_Φ, K_Θ) and u_{i1}, u_{i2}, is the short notation for $u_{\text{inter},\nu}$, $u_{\text{inter},(1-\nu)}$, respectively. The effects of the interlayer backscattering interactions, included on the new matrix of Eq. (69) (which we denote by N_Θ), shift the poles of the boson propagators. The low-energy collective modes now are given by

$$\omega_\pm^2(\mathbf{q}) = \pi^2\frac{A}{2}\left[1 \pm \sqrt{1-\frac{4D}{A^2}}\right], \quad (70)$$

where

$$A = q_x^2\text{Tr}(K_\Phi K_\Theta) + 2N_\Theta^{11}K_\Phi^{22} + 2\text{Re}\{K_\Phi^{12}N_\Theta^{21}\}, \quad (71)$$

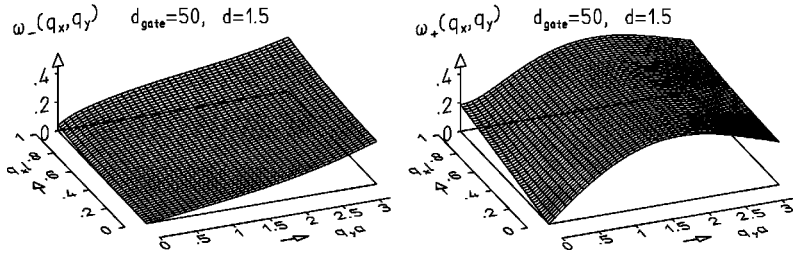

FIG. 7. The collective modes of the bilayer QH smectic interlayer coherent phase, for the case of $K_{\Phi/\Theta}(x,j)$ of Eqs. (23) and (25) and $N=2$, $\nu\approx 1/2$ and $a=5.8l$, are shown. $\omega_+(q_x,q_y)$, the right panel, is of the form of a spatially anisotropic two-dimensional ferromagnet, $\omega_+^2(\mathbf{q})\sim Kq_x^2+uq_y^2$. The $\omega_-(q_x,q_y)$ collective mode vanishes only for $q_y\to 0$ *and* $q_x\to 0$ when nonlocal contributions to the interaction coefficients are accounted for.

$$D=\det(K_\Phi)\{q_x^4\det(K_\Theta)+2N_\Theta^{22}K_\Theta^{11}+\det(N_\Theta) -2q_x^2\mathrm{Re}[K_\Theta^{12}N_\Theta^{21}]\}. \tag{72}$$

These low-energy collective modes are shown in Fig. 7.

As before, the case of balanced filling fraction can be described in a more transparent way using the scalar couplings $\tilde{K}_\Phi$, $\tilde{K}_\Theta$ of Eqs. (32) and (33). For this case the low-energy collective modes have the form

$$\omega_\pm^2(\mathbf{q})=\pi^2\tilde{K}_\Phi(\mathbf{q})\{q_x^2\tilde{K}_\Theta(\mathbf{q})+2u_{i1}[1+\cos(q_y a/2)]\}. \tag{73}$$

In this formulation one of the gapless modes is located at the edge of the Brillouin zone, which is now doubled, at $q_y=2\pi/a$. In the extended Brillouin zone we use for balanced bilayers the $\omega_-(\mathbf{q})$ softmode appears for $q_y\to 0$, whereas the $\omega_+(\mathbf{q})$ softmode appears as $q_y\to 2\pi/a$. The two modes have the following behaviors:

$$\omega_-^2(\mathbf{q})\approx\pi^2\tilde{K}_\Phi''(\mathbf{0})q_y^2[\tilde{K}_\Theta(\mathbf{0})q_x^2+4u_{i1}], \tag{74}$$

$$\omega_+^2(\mathbf{q})\approx\pi^2\tilde{K}_\Phi\left(\frac{2\pi}{a}\right)\left[\tilde{K}_\Theta\left(\frac{2\pi}{a}\right)q_x^2+\frac{u_{i1}a^2}{4}\left(q_y-\frac{2\pi}{a}\right)^2\right]. \tag{75}$$

Similar results can be obtained using the matrix formulation for general ν and become equivalent for $\nu=1/2$. There is no qualitative change in the collective mode structure when $\nu\neq 1/2$.

The interlayer phase-coherent smectic state is characterized by a finite value of the following order parameter,

$$\Psi(\mathbf{r})=\langle\psi_T^\dagger(\mathbf{r})\psi_B(\mathbf{r})\rangle=\frac{1}{2\pi}\langle e^{-2i\Theta(\mathbf{r})}\rangle\approx\frac{1}{2\pi}e^{-1/2\langle 4\Theta^2(\mathbf{r})\rangle}, \tag{76}$$

where $\psi_T^\dagger$, ψ_B are fermion creation and annihilation for the top and bottom layers, respectively. We now show that $\langle\Theta^2(\mathbf{r})\rangle$ is finite. We discuss only the case of balanced bilayers, using the alternative formulation which is more transparent. We find that

$$\langle\Theta_j^2\rangle=\int\frac{d^2q}{\frac{(2\pi)^2}{a/2}}\frac{d\omega}{2\pi} \times\frac{\tilde{K}_\Phi(\mathbf{q})}{\frac{\omega^2}{\pi^2}+\tilde{K}_\Phi(\mathbf{q})\left[q_x^2\tilde{K}_\Theta(\mathbf{q})+2u_{i1}\left[1+\cos\left(\frac{q_y a}{2}\right)\right]\right]} \approx\frac{a}{16\pi}\int_{-2\pi/a}^{2\pi/a}dq_y\sqrt{\frac{\tilde{K}_\Phi(q_y)}{\tilde{K}_\Theta(q_y)}} \times\ln\left[\frac{2\tilde{K}_\Theta(q_y)(1/l)}{u_{i1}(1+\cos(q_y a/2))}\right]. \tag{77}$$

In Eq. (77) we have introduced an upper short distance cutoff $1/\ell$ for the q_x integration. Interlayer backscattering interactions have cutoff the infrared divergence of the q_x integration, making the integral finite and establishing particle-hole pair condensation. In this state the $U(1)$ symmetry associated with conservation of total charge difference N_T-N_B between top and bottom layers is broken.

We conclude on the basis of this analysis that interlayer backscattering will drive the Hartree-Fock bilayer smectic state to a state which has both broken translational and orientational symmetry *and* spontaneous interlayer phase coherence along the edges. We expect this state to exhibit giant interlayer tunneling conductance anomalies at low-bias voltages, similar to those that have been seen in the $N=0$ Landau-level in bilayers. Although these states have a charge gap that we discuss below and should exhibit the quantum Hall effect, we expect that they will exhibit strongly anisotropic dissipative transport at finite temperatures. Their two gapless collective modes arise, because they have broken translational and orientational symmetry and spontaneous interlayer phase coherence. We also note that the quantum character of these bilayer smectic states is quite distinct from the quantum smectics discussed previously for the single-layer case. For instance, the long-wavelength behavior of the quantized collective mode $\omega_-(q_x,q_y)$ changes from being proportional to $|q_xq_y|$ to being proportional to $|q_y|$ only when spontaneous interlayer phase coherence is present; locking the phase difference between different layers quali-

tatively increases the cost of independent position fluctuations. The long-wavelength behavior of the $\omega_+(q_x,q_y)$ collective mode is that of an anisotropic superfluid. As in the case of uniform states, spontaneous interlayer phase coherence is equivalent to electron-hole pair superfluidity, but the broken orientational symmetry of the smectic state causes this superfluid to have orientation dependent stiffness.

It seems quite possible that the order parameter that characterizes the broken orientational and translational symmetry of these states will be driven to zero when interlayer interactions are sufficiently strong. Indeed this is suggested[15,16] by mean-field calculations. We are unable to estimate where this transition takes place using the methods of this paper.

2. Coherent smectic state specific heat

The internal energy of the bilayer smectic phase-coherent (SPC) state will be dominated at low energies by the contribution from the $\omega_-(\mathbf{q})$ mode. The leading contribution to the integral for the internal energy comes from the region of small $\mathbf{q}$. The q_x integral now has a natural infrared cutoff, however, at $\sqrt{u_{i1}/\tilde{K}_\Theta(\mathbf{0})}$. It follows that the internal energy is given for small u by

$$U \approx \frac{2a}{\pi^3\sqrt{\tilde{K}_\Theta(0)\tilde{K}''_\Phi(0)}} T^2\zeta(2)\ln\left(\frac{\tilde{K}_\Theta(0)}{4u_{i1}}\frac{1}{al}\right), \quad (78)$$

and the specific heat will now be linearly dependent on T. The specific heat anomaly noted previously for the bilayer smectic is suppressed when interlayer coherence is established, even though broken translational and orientational symmetry are still present.

3. The Wigner crystal state

Intralayer backscattering interactions take the form

$$\hat{O}_{\rm intra} = -u\{\exp[i(2k_F x+\Phi_j^2-\Phi_j^1+\Phi_{j+1}^1-\Phi_{j+1}^2)] \times \exp[i(-\Theta_j^2-\Theta_j^1+\Theta_{j+1}^1+\Theta_{j+1}^2)]+\text{H.c.}\}, \quad (79)$$

where the oscillatory dependence on coordinate along the edge which we have exhibited explicitly follows from our earlier field operator definitions. This interaction dominates only at quite large layer separations. When it does it drives the system to a state which has periodicity along the stripe edges as well as across the stripes. Since, the wavelength along the stripe is $4\pi l^2/a$, and since the periodicity along the direction perpendicular to the stripes is a, this state will contain one electron per layer per two-dimensional unit cell. We therefore identify this state as a bilayer Wigner crystal (WC) state.

D. Gap estimates for bilayer stripe states

The most important conclusion from the above calculations is that interlayer Coulomb backscattering interactions are always relevant in bilayer stripe states. *The gapless bilayer stripe state can never be the true ground state.* Since the bare matrix elements associated with these interactions are often quite small, however, they will often be important only at low temperatures. As we explain below, we believe that Coulomb interactions will most often drive the system either to an isotropic coherent state or to a smectic coherent state. Both states will have a charge gap and an integer quantum Hall effect. In this section we estimate the size of this gap, and hence the temperature above which we expect the phenomenology of these states to crossover from quantum Hall behavior to stripe-state behavior.

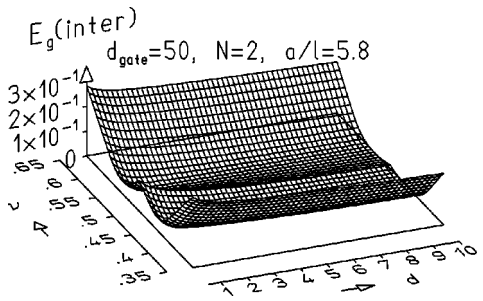

FIG. 8. Estimated charge gap due to interlayer backscattering interactions. These interactions are always relevant and lead, in the absence of interlayer tunneling, to states with spontaneous interlayer phase coherence.The energy scale in this figure is $\sim e^2/\epsilon\ell$ which is $\sim k_B 50$ K for a typical higher Landau-level experiment. The energies should be reduced to account for screening from inter-Landau-level transitions that we have not included in our calculations.

Our estimates are built on bare matrix elements whose evaluation we discuss below and on the scaling dimension calculations discussed above. Given dimensionless interlayer and intralayer backscattering interactions $u_{\rm inter}$ and $u_{\rm intra}$, we can estimate the gap by integrating the RG flow equations to obtain

$$E_g^{e/a}(u_{e/a}) = b^{-1}E_g^{e/a}(b^{2-\Delta_{e/a}}u_{e/a}), \quad (80)$$

where the superscripts and subscripts e/a are used for inter-layer and intra*a*layer interactions, respectively. When the interactions become of order 1 on the renormalized energy scale ($b^{2-\Delta}u=1$), the energy gap should be roughly equal to the renormalized characteristic Coulomb energy E_c, giving

$$E_g(u) = (U/E_c)^{1/(2-\Delta)}E_c, \quad (81)$$

where $U=uE_c$ is the microscopic high-energy-scale backscattering interaction strength. The ν dependence of the gap enters through U, and through the scaling dimensions. Both effects conspire to strongly reduce the gap magnitude near half filling. Taking $E_c=0.3e^2/l$, approximately the maximum correlation energy per electron in a partially filled Landau level, the resulting gaps for $N=2$ and $d_{\rm gate}=50l$, are shown as a function of filling fraction and distance between layers in Figs. 8–10. We notice that the gap resulting from the intralayer backscattering interaction is very small near half filling, dropping below the range accessible to dilution fridges over most of the filling factor shown in this figure. On the other hand the gap resulting from the interlayer back-

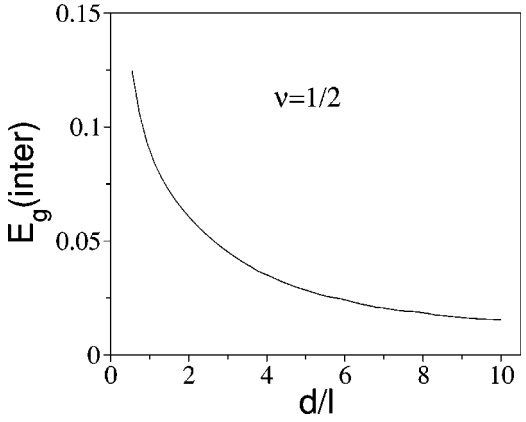

FIG. 9. Estimated charge gap due to interlayer backscattering interactions, for balanced bilayers ($\nu=1/2$ in each layer), as a function of layer separation. This dependence is extracted from Fig. 8 and shown here for clarity.

scattering interactions is not as small and remains reasonably large out to large values of the interlayer separation d. Recalling that this interaction is proportional to $R_1^\dagger L_1 L_2^\dagger R_2$, we see that when this interaction is strong it favors interlayer phase coherence along each stripe edge and that when it is very strong it leads to condensation of the field $\Theta_j^1+\Theta_j^2$ to a value independent of j. Since Θ_j^λ is by definition the phase difference between left- and right-going fermion fields at the (j,λ) stripe edge, and since the layer indices of right- and left-going fermions is opposite at $\lambda=1$ and $\lambda=2$ stripe edges, what is condensing when this interaction is strong is the phase difference between fermions in opposite layers. In other words, *the state that occurs in the strong interedge backscattering limit has spontaneous interlayer phase coherence*. States with interlayer phase coherence and stripe order can occur as local and even global minima of Hartree-Fock energy functionals. Coupled with the irrelevance of intralayer backscattering interactions at small layer separations in the bilayer case, our analysis suggests that they can be the ground states of bilayer quantum Hall systems in high Landau-levels.

For intralayer backscattering, the bare backscattering interaction matrix element has both direct and exchange contributions, while interlayer backscattering has only a direct contribution. An elementary calculation using the Landau gauge basis states leads to the following explicit expressions that were used to obtain gap estimates.

Same-layer direct

$$k_1 l^2 = Y_1 + Ql^2, \quad k_2 l^2 = Y_2 - Ql^2, \tag{82}$$

$$k_3 l^2 = Y_1, \quad k_4 l^2 = Y_2, \tag{83}$$

and

$$\langle Y_1+Ql^2, Y_2-Ql^2|V|Y_1,Y_2\rangle = \frac{1}{2\pi} e^{-a^2\nu^2/2l^2} \int dq_x e^{-q_x^2 l^2/2} e^{-iq_x a} V_s^n(q_x,Q), \tag{84}$$

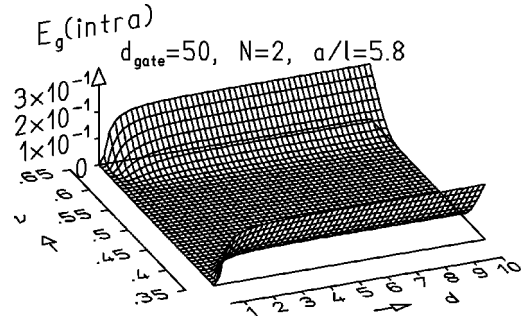

FIG. 10. Estimated charge gap that would result from intralayer backscattering interactions in the bilayer case. When the scaling dimension is larger than two, the gap vanishes. Intralayer interactions are more important than interlayer interactions only at very large layer separations. The energy scale in this figure is $e^2/\epsilon\ell$.

same-layer exchange

$$k_2 l^2 = Y_1 + Ql^2, \quad k_1 l^2 = Y_2 - Ql^2, \tag{85}$$

$$k_3 l^2 = Y_1, \quad k_4 l^2 = Y_2, \tag{86}$$

$$\langle Y_2-Ql^2, Y_1+Ql^2|V|Y_1,Y_2\rangle = \frac{1}{2\pi} e^{-a^2/2l^2} \int dq_x e^{-q_x^2 l^2/2} e^{-iq_x a\nu} V_s^n(q_x, a/l^2), \tag{87}$$

different-layer direct

$$k_1 l^2 = Y_1 + Ql^2, \quad k_2 l^2 = Y_1, \tag{88}$$

$$k_3 l^2 = Y_1, \quad k_4 l^2 = Y_1 + Ql^2, \tag{89}$$

$$\langle Y_2, Y_1|V|Y_1,Y_2\rangle = \frac{1}{2\pi} e^{-a^2\nu^2/2l^2} \int dq_x e^{-q_x^2 l^2/2} V_D^n(q_x,Q), \tag{90}$$

where the subscripts S and D refer to two-dimensional Fourier transforms of the Coulomb interactions between electrons in same and different layers. We see in Figs. 8–10 that the importance of interlayer interactions diminishes rather slowly with layer separation, leading to sizable integer quantum Hall gaps out to large layer separations.

Our results for the energy gaps are summarized in Fig. 11 by a schematic phase diagram intended to represent predicted experimental findings in very high mobility bilayer systems at dilution refrigerator temperatures. This phase diagram was constructed from a recipe specified below. Different regions of the phase diagram as a function of layer separation d/l and imbalance, characterized by ν, are identified as exhibiting the behavior of one of the following phases. The bilayer smectic state is a state with no integer quantum Hall effect, and anisotropic transport. The coherent bilayer smectic state will have an integer quantum Hall effect but will still have anisotropic transport at finite temperature. The bilayer Wigner crystal state will have an integer quantum Hall effect with an odd integer quantized Hall conductivity. We predict bilayer smectic state behavior when neither inter-

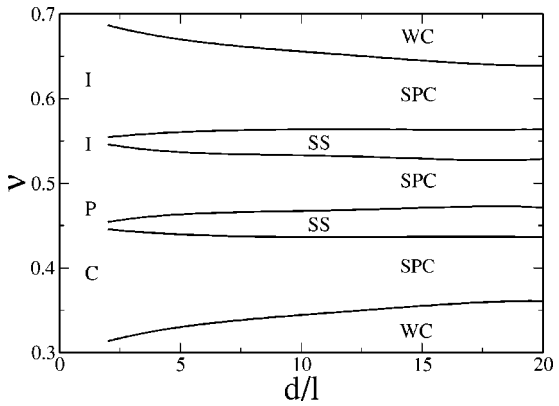

FIG. 11. Apparent phase diagram predicted for experimental studies of high mobility bilayer systems at dilution fridge temperatures. The various phases in this illustration have qualitatively different transport properties. These calculations are for stripe states in the $N=2$ orbital Landau level ($a=5.8\ell$), with weak remote-gate screening ($d_{\text{gate}}=50\ell$). It is possible to explore the phase diagram experimentally in a single sample, since both the top layer filling factor ν and the normalized interlayer separation d/ℓ, are altered when the charge imbalance and total electron density are changed by using front and back gates in combination. For interlayer spacing d less than approximately 1.5ℓ and any charge imbalance, we expect the bilayer to be in an isotropic interlayer phase coherent state which has a large gap, integer quantum Hall effect and isotropic transport properties. Anisotropic states are expected only for more widely spaced layers, $d>1.5\ell$. For strongly unbalanced layers (ν far from 1/2) we expect anisotropic WC states to appear because of intralayer backscattering interactions, just as they do in the single-layer case. These states will exhibit a quantum Hall effect with an odd integer quantized Hall conductivity. Stripe (smectic metal) states (SS) tend to occur when each layer has a filling factor close to $\nu=1/2$, but as in the single-layer case these states are never the true ground states. Smectic metal states show anisotropic transport, but do not show an integer quantum Hall effect. Interlayer backscattering interactions always induce charge gaps but these are sometimes too small to be observable at a typical dilution fridge temperatures which we take to be $0.001e^2/\epsilon\ell$. Regions with an estimated charge gap larger than this value are labeled as SPC state regions in the phase diagram. Smectic phase-coherent states have an odd integer quantum Hall effect, and are expected to have transport properties which are much more anisotropic than those of the anisotropic Wigner crystal states. This state should also exhibit giant interlayer tunneling conductance anomalies at low-bias voltages.

layer nor intralayer backscattering interactions produce a gap larger than $0.001e^2/\epsilon\ell$. We judge that a gap smaller than this size would not produce observable effects in a typical dilution fridge experiments. Interlayer backscattering interactions are much more effective than intralayer interactions in producing gaps, because they are strongly relevant. We predict bilayer Wigner crystal behavior when the intralayer backscattering yields the largest gap and a gap that exceeds our minimum value. These states are expected only when the charge imbalance is large or the layer separation is quite large. We predict bilayer coherent smectic states when interlayer backscattering produces the largest gap, provided again that it exceeds our minimum value. Because the intralayer interactions are strongly relevant, observable gaps are expected out to very large layer separations, an unexpected result of our analysis. The interval of charge imbalance where stripe (smectic metal) states are expected expands only modestly with layer separation, but *is* sensitive to the orbital index N of the Landau-levels, since nodes in the orbital wave functions can cause the bare backscattering matrix element to vanish at particular N-dependent values of ν. The details of boundaries separating stripe state and stripe-phase-coherent regions of this phase diagram will be quite different for different values of N. As we have emphasized, our approach is reliable only when quantum fluctuations around the mean-field stripe state of the Hartree-Fock theory are weak. For small layer separations the charge gaps start to become comparable to the underlying microscopic energy scales. In this regime we expect that the ground state is actually an isotropic coherent bilayer state, but are unable to provide a reliable quantitative estimate of the layer separation at which this transition occurs.

V. DISCUSSION AND CONCLUSIONS

In this paper, we have studied double-layer quantum Hall systems at odd integer total filling fractions. Mean-field theory predicts that these systems can form striped ground states. This observation serves as the starting point for our work. The Hilbert space in which the low-energy excited states of mean-field bilayer stripe states reside may be mapped to those of an infinite set of coupled-Luttinger-liquids, one for each stripe, allowing us to borrow bosonization techniques from the literature on one-dimensional electron systems. Quantum fluctuations around the mean-field stripe state are conveniently described in terms of the Bose quantum fields that can be interpreted as representing charge density and position fluctuations along each stripe edge. The interactions that control quantum fluctuations in the electron ground state include both forward-scattering terms which contribute to quadratic interactions in the boson Hamiltonian and weak, but more complicated backscattering terms. The coupled-Luttinger-liquid model obtained when the backscattering interactions are neglected is not of the standard form, because both charge and position terms in the effective Hamiltonian have a matrix character, and because the energy cost of fluctuations in which stripes move collectively is small when the stripes are not pinned. We find that the latter property leads to fermion spatial correlations whose decay is faster than any power law, to a specific heat that vanishes less quickly than T for $T\rightarrow 0$, and to a tunneling density of states that vanishes faster than any power law for $E\rightarrow 0$. These properties of bilayer stripe states are similar to properties established previously for single layers by Lopatnikova *et al.* and Barci *et al.* There is no limit in which bilayer stripe quantum Hall states can be treated as a system of weakly-coupled-Luttinger liquids.

We address the role played by intralayer and interlayer backscattering interactions by evaluating their perturbative renormalization group scaling dimensions, following an approach two of us have taken previously for the case of single-layer stripe states.[19] In the single-layer case we reached the conclusion that these interactions are always rel-

evant, and that they are likely to drive the system to a Wigner crystal state with an energy gap. Estimates of the size of this gap based on bare backscattering matrix elements and scaling dimensions gave extremely small values, however, consistent with the observation of stripe-state phenomenology at temperature scales that could be reached experimentally. Since other researchers have reached different conclusion about the relevance of backscattering interactions in single-layer systems, it is worthwhile in stating the conclusions that we have reached in the present work to emphasize once again the philosophy that underpins our calculations and explain why we have considerable confidence in the conclusions we reached previously.

Our identification of a low-energy Hilbert space in which it is possible to derive a simplified many-electron Hamiltonian is based on the experimental discovery of stripe states and on evidence from experiment that the true ground state is energetically very close to the mean-field theory ground state. In our view the most convincing evidence in this regard is the ability[32] of the Hartree-Fock theory to accurately predict the dependence of the stripe state orientation on in-plane field strength, quantum well width, and other microscopic parameters. In single-layer systems, quantum fluctuations are important only at low-energies and long-length scales. When mean-field theory accurately describes the microscopic length scale physics, we can use the elementary excitations of the Hartree-Fock stripe state to identify the Hilbert space of low-energy excitations, and confidently use bare interaction matrix elements to estimate forward-scattering and backscattering interaction parameters. The issue of quantum stability of smectic states in single-layer systems has received interest partly, because it is closely related to the possible existence[33,27,34] of freely sliding analogs of the Kosterlitz-Thouless phase in stacked two-dimensional XY models. Although it is certainly clear[27] that the interacting Luttinger-liquid fixed-point actions exist for which backscattering interactions are irrelevant, this observation is not sufficient to decide on their relevance in the case of quantum Hall stripe states. Crudely speaking, irrelevance in the case of repulsive interactions requires[19,28] that the forward-scattering interaction strength decay in a strongly nonmonotonic way with edge separation. For single-layer systems Fertig and collaborators[35] have estimated forward-scattering amplitudes using an approach that goes beyond the weak-coupling approximations we employ, doing so, however, in a partially *ad hoc* manner by fitting their model to collective modes evaluated in a time-dependent Hartree-Fock approximation. Their conclusion on the relevance of backscattering interactions is opposite to ours. The source of the discrepancy may be traced to the broken particle-hole symmetry in the half filled Landau-level Hartree-Fock approximation Wigner crystal state that they use to extract strong-coupling interaction parameters. *For a single-layer stripe state, backscattering interactions can be irrelevant at* $\nu=1/2$ *only if the true ground state breaks particle-hole symmetry.* Since stable stripe states are most likely to occur at $\nu=1/2$ and Landau-level mixing (neglected in these theories) also works against stripe-state stability, we believe that stripe states are never stable in single-layer quantum Hall systems. This raises an interesting question. Could there be another class of as yet undetected phase transitions that occur in the quantum Hall regime either in the high-N stripe-state regime, or perhaps even for lower N where stripe states do not occur? Broken particle-hole symmetry at $\nu=2$ would imply a finite-temperature phase transition in the 2D Ising universality class, for which the deviation of the Hall conductivity at $\nu=1/2$ from $e^2/2h$ could be taken as the order parameter. There is certainly no evidence for such a phase transition in experiment, although it might be washed out by disorder[36] even if it occurred. In any event, broken particle-hole symmetry in the ground state would require that a phase transition occur between the high-temperature stripe state of Hartree-Fock theory that does not have broken particle-hole symmetry and a low-temperature stripe state, in which particle-hole symmetry is broken and backscattering is irrelevant. In light of the evidence that fluctuation corrections to the Hartree-Fock ground state are weak, we believe that the simpler conclusion of our earlier work is more likely to be correct, namely, that particle-hole symmetry is not broken and that the smectic state is not stable.

As we have emphasized several times, the approach we have taken does not lead to completely standard coupled-Luttinger-liquid properties, because some interaction parameters vanish for $q_y \to 0$. In particular, the decay properties of fermion correlation functions at large distances, and of the tunneling density of states at small energies, are faster than power laws. This conclusion of our analysis follows from the broken translational symmetry in the stripe state which makes its energy functional invariant under a simultaneous translation of all stripes. Barci *et al.*,[24] have argued that this unusual property might signal a failure of the perturbative renormalization group transformation we have used, which rescales spatial coordinates along the stripe edges but not across them. Our approach is dictated, we believe, by the nature of the mean-field state that is suggested by the Hartree-Fock theory and by experiment. When backscattering is neglected, the quadratic Hamiltonian of the system scales as q_x^2 at *all* q_y values. Because the chiral stripe edges are discrete, $|q_y|$ is restricted to a Brillouin zone and there is no simple power-law dependence for q_y that applies throughout its range. The Luttinger-liquid action will therefore not be invariant under any transformation that scales the y coordinate. We do not see any alternative to our perturbative RG approach to account for the neglected backscattering terms. In the present analysis of bilayer stripe states, we have found it convienent to group the stripe edges in pairs with opposite chirality, and localized near the same planar position in opposite layers. In this language,the fluctuations of the pair can be separated into fluctuations of the position and the charge density of a stripe pair. We have found that the charge-density fluctuations are more violent and they are responsible for the unusual properties of these strongly coupled-Luttinger liquids: the rapid decay of the correlation functions, the strong suppression of the single-particle density of states, and the enhancment of the specific heat at low temperatures. The special features of long-wavelength shear fluctuations in smectic systems, which lead to collective modes with dispersion $\omega^2 \sim q_x^2[q_y^2+q_x^4]$ for small q_x and q_y

and, in particular, with $\omega \sim q_x^3$ at $q_y = 0$, do play a minor role in the calculation of some correlation functions and the specific heat. These features are not captured by our renormalization scheme. However, it is intended only to shed light only on the stability of the smectic state. It obtains well-defined values for backscattering operator scaling dimensions without this higher order in wave vector information on scattering amplitudes.

Our conclusions concerning the nature of the true ground state could, in principle, be altered if it were possible to extend the perturbative RG analysis to higher order. Indeed this must happen when our analysis is applied to low index Landau levels, in which stripe states do not occur. We do not believe, however, that the unusual correlation functions signal a greater likelihood of this eventuality than normally applies to lowest-order perturbative RG calculations. In practice, the microscopic backscattering amplitudes treated perturbatively are sufficiently weak in high Landau-levels that our lowest-order calculations seem likely to describe what happens down to the lowest-temperatures available experimentally, at least when the Landau-levels are close to half-odd-integer filling factor per layer. Well away from $\nu = 1/2$, the Hartree-Fock theory suggests that the true ground state is composed of bubbles rather than stripes, a transformation in the physics that our analysis does not recoginize. In our view the approach we have taken should be trusted when experimental evidence suggests that the physics at low energies is described by the stripe states of the Hartree-Fock theory.

We find here that the role of backscattering interactions is quite different in the bilayer case compared to the single-layer case. At very large layer separations, the single-layer case in which stripe state physics occurs down to very low temperatures for $\nu \sim 1/2$ is recovered. However, already for layer separations $\sim 10\ell$, we find that interlayer backscattering interactions which drive the system toward a state with spontaneous interlayer phase coherence along the edges become important and lead to a state with a substantial charge gap. Our prediction of odd integer quantum Hall effects with anisotropic finite-temperature transport coefficients in surprisingly widely separated bilayer systems is an important result of this paper. This conclusion about the properties of spontaneously coherent stripe states in the absence of interlayer tunneling differs from that reached by Fertig and collaborators who, incorrectly in our view, ignore interedge coupling in considering the properties of coherent stripes. Interestingly, intralayer backscattering interactions that drive the system toward a Wigner crystal state are irrelevant in this regime. *We conclude that stripe states are stable in bilayer quantum Hall systems, unlike the single-layer case, but have an excitation gap unlike smectic metals.* It seems likely that for very small layer separations, backscattering interactions will drive the system toward a uniform charge-density state with interlayer coherence, although our perturbative approach is not able to offer any substantial guidance in deciding this question.

The study of stripe-state physics in single-layer quantum Hall systems requires samples of exceptional quality, beyond that required for studies of fractional quantum Hall physics with the lower index partially filled Landau-levels which can be studied at higher magnetic fields. It is still not possible to create bilayer quantum Hall systems with disorder that is as weak as that in single-layer quantum Hall systems. Nevertheless, recent samples appear to be of a quality that opens the physics of stripe states in bilayer systems up to experimental study. We expect on the basis of this work, and of previous theoretical work, that the physics will be rich, with much potential for surprises beyond the properties anticipated here.

ACKNOWLEDGMENTS

The authors are grateful for helpful and stimulating interactions with Dave Allen, Alan Dorsey, Rene Côté, Herb Fertig, Eduardo Fradkin, Steve Kivelson, Tom Lubensky, Tilo Stroh, Alexei Tsvelik, and Carlos Wexler. Work in Austin was supported by the National Science Foundation under Grant No. NSF-DMR-0115947. Work in Santa Barbara was supported by NSF Grants Nos. DMR-0210790 and Phy-9907949.

[1] M.P. Lilly, K.B. Cooper, J.P. Eisenstein, L.N. Pfeiffer, and K.W. West, Phys. Rev. Lett. **82**, 394 (1998); **83**, 824 (1999).

[2] R.R. Du, D.C. Tsui, H.L. Stormer, L.N. Pfeiffer, K.W. Baldwin, and K.W. West, Solid State Commun. **109**, 389 (1999); W. Pan, R.R. Du, H.L. Stormer, D.C. Tsui, L.N. Pfeiffer, K.W. Baldwin, and K.W. West, Phys. Rev. Lett. **83**, 820 (1999).

[3] M. Shayegan, H.C. Manoharan, S.J. Papadakis, and E.P. DePoortere, Physica E **6**, 40 (2000).

[4] For a recent review see J.P. Eisenstein, Solid State Commun. **117**, 123 (2001).

[5] For a recent review see M.M. Fogler, cond-mat/0111001 (unpublished).

[6] A.A. Koulakov, M.M. Fogler, and B.I. Shklovskii, Phys. Rev. Lett. **76**, 499 (1996); Phys. Rev. B **54**, 1853 (1996); M.M. Fogler and A.A. Koulakov, *ibid.* **55**, 9326 (1997).

[7] R. Moessner and J.T. Chalker, Phys. Rev. B **54**, 5006 (1996).

[8] E.H. Rezayi, F.D.M. Haldane, and K. Yang, Phys. Rev. Lett. **83**, 1219 (1999); F.D.M. Haldane, E.H. Rezayi, and K. Yang, *ibid.* **85**, 5396 (2000).

[9] N. Shibata and D. Yoshioka, Phys. Rev. Lett. **86**, 5755 (2001).

[10] For a review on experimental research see J.P. Eisenstein in *Perspectives in Quantum Hall Effects*, edited by S. Das Sarma and A. Pinczuk (Wiley, New York, 1997); for a review on theoretical research see S.M. Girvin and A.H. MacDonald, in the same volume.

[11] H. Fertig, Phys. Rev. B **40**, 1087 (1989); A.H. MacDonald, P.M. Platzman, and G.S. Boebinger, Phys. Rev. Lett. **65**, 775 (1990); K. Moon, H. Mori, K. Yang, S.M. Girvin, A.H. MacDonald, L. Zheng, D. Yoshioka, and S.-C. Zhang, Phys. Rev. B **51**, 5138 (1995); K. Yang, K. Moon, L. Belkhir, H. Mori, S.M. Girvin,

A.H. MacDonald, L. Zheng, and D. Yoshioka, *ibid.* **54**, 11 644 (1996).

[12] S.Q. Murphy, J.P. Eisenstein, G.S. Boebinger, L.N. Pfeiffer, and K.W. West, Phys. Rev. Lett. **72**, 728 (1994).

[13] I.B. Spielman, J.P. Eisenstein, L.N. Pfeiffer, and K.W. West, Phys. Rev. Lett. **84**, 5808 (2000); *ibid.* **87**, 036803 (2001); M. Kellogg, I.B. Spielman, J.P. Eisenstein, L.N. Pfeiffer, and K.W. West, Phys. Rev. Lett. **88**, 126804 (2002). These experiments have been reviewed and discussed recently by J.P. Eisenstein, Phys. World **14**(6), 30 (2001); B.G. Levi, Phys. Today **54**(1), 15 (2001); and S.M. Girvin, in *Proceedings of 11th International Conference on Recent Progress in Many-Body Theories*, edited by R.F. Bishop *et al.* (World Scientific, Singapore, 2002).

[14] L. Balents and L. Radzihovsky, Phys. Rev. Lett. **86**, 1825 (2001); A. Stern, S.M. Girvin, A.H. MacDonald, and N. Ma, *ibid.* **86**, 1829 (2001); M.M. Fogler and F. Wilczek, *ibid.* **86**, 1833 (2001); J. Schliemann, S.M. Girvin, and A.H. MacDonald, *ibid.* **86**, 1849 (2001); E. Demler, C. Nayak, and S. Das Sarma, *ibid.* **86**, 1853 (2001); K. Yang, *ibid.* **87**, 056802 (2001); Y.N. Joglekar and A.H. MacDonald, *ibid.* **87**, 196802 (2001).

[15] L. Brey and H.A. Fertig, Phys. Rev. B **62**, 10 268 (2001).

[16] R. Côté and H.A. Fertig, Phys. Rev. B **65**, 085321 (2002).

[17] E. Demler, D.-W. Wang, S. Das Sarma, and B.I. Halperin, Solid State Commun. **123**, 243 (2003).

[18] W. Pan, H.L. Stormer, D.C. Tsui, L.N. Pfeiffer, K.W. Baldwin, and K.W. West, Phys. Rev. B **64**, 121305 (2001).

[19] A.H. MacDonald and M.P.A. Fisher, Phys. Rev. B **61**, 5724 (2000).

[20] Comparison between the energies of mean-field stripe states and Laughlin-like correlated fluid variational states are, however, quite successful in predicting when *stripe* and related *bubble* states occur. See, for example, R.M. Lewis, P.D. Ye, L.W. Engel, D.C. Tsui, L.N. Pfeiffer, and K.W. West, cond-mat/0205200 (unpublished).

[21] A.O. Gogolin, A.A. Nersesyan, and A.M. Tsvelik, *Bosonization and Strongly Correlated Systems* (Cambridge University Press, Cambridge, 1998); *Bosonization*, edited by M. Stone (World Scientific, Singapore, 1994), a collection of reprints.

[22] E. Fradkin and S.A. Kivelson, Phys. Rev. B **59**, 8065 (1999). This paper assumes that the fluctuating positions of the stripes provide degrees of freedom additional to those provided by stripe-edge particle-hole excitations. More recent work by these authors and collaborators starts from the same point as Ref. 19, but regards the model's interaction parameters as phenomenological, rather than attempting to estimate them.

[23] A. Lopatnikova, S.H. Simon, B.I. Halperin, and X.-G. Wen, Phys. Rev. B **64**, 155301 (2001).

[24] Daniel G. Barci, Eduardo Fradkin, Steven A. Kivelson, and Vadim Oganesyan, Phys. Rev. B **65**, 245319 (2002); Daniel G. Barci and Eduardo Frakdin, *ibid.* **65**, 245320 (2002).

[25] C. Wexler and A.T. Dorsey, Phys. Rev. B **64**, 115312 (2001); **60**, 10 971 (1999).

[26] Leo Radzihovsky and Alan T. Dorsey, Phys. Rev. Lett. **88**, 216802 (2002).

[27] V.J. Emergy, E. Fradkin, S.A. Kivelson, and T.C. Lubensky, Phys. Rev. Lett. **85**, 2160 (2000); E. Fradkin, S.A. Kivelson, E. Manousakis, and Kwansik Nho, *ibid.* **84**, 1982 (2000).

[28] The limit $d_{\text{gate}} \to \infty$ has been carefully discussed elsewhere for the single-layer case. A.H. MacDonald and M.P.A. Fisher in *Lecture Notes in Physics*, edited by Tobias Brandes, Interactions and Trasport Properties of Low-Dimensional Systems, Vol. 544 (Springer, New York, 2000).

[29] For an introduction to symmetry related properties of smectic energy functionals see P.M. Chaikin and T.C. Lubensky, *Principles of Condensed Matter Physics* (Cambridge University Press, Cambridge, 1995); for applications of RG techniques to quantum Hall liquid crystals, see also S. Scheidl and F. von Oppen, Europhys. Lett. **55**, 260 (2001).

[30] Emiliano Papa and Alexei M. Tsvelik, Phys. Rev. B **63**, 085109 (2001); **60**, 12 752 (1999).

[31] T. Jungwirth, A.H. MacDonald, L. Smrčka, and S.M. Girvin, Phys. Rev. B **60**, 15 574 (1999). See also Daijiro Yoshioka, J. Phys. Soc. Jpn. **70**, 2836 (2001); and T. Stanescu, I. Martin, and P. Phillips, Phys. Rev. Lett. **84**, 1288 (2000).

[32] T. Jungwirth, A.H. MacDonald, L. Smrčka, and S.M. Girvin, in *Proceedings of ICPS25*, edited by N. Miura (Springer-Verlag, Berlin, 2001), p. 933; T. Jungwirth, A.H. MacDonald, L. Smrčka, and S.M. Girvin, Phys. Rev. B **60**, 15 574 (1999).

[33] C.S. O'Hern, T.C. Lubensky, and J. Toner, Phys. Rev. Lett. **83**, 2745 (1999).

[34] S.L. Sondhi and Kun Yang, Phys. Rev. B **63**, 054430 (2001).

[35] Hangmo Yi, H.A. Fertig, and R. Côté, Phys. Rev. Lett. **85**, 4136 (2000); R. Côté, Phys. Rev. B **62**, 1993 (2000).

[36] Y. Imry and M. Wortis, Phys. Rev. B **19**, 3580 (1979).